REPORT DOCUMENTATION PAGE

AFRL-SR-AR-TR-03-

0169

1. AGENCY USE ONLY *(Leave Blank)*	2. REPORT DATE	3. REPORT TYPE AND DATES COVERED
	April 23, 2003	Final - November 1999 - December 2003

4. TITLE AND SUBTITLE
Real-time Measurements of Reactive Chlorine and Carbon Dioxide in Rocket Plumes

5. FUNDING NUMBERS
F49620-99-1-0131

2303/EX
61102F

6. AUTHORS
Darin W. Toohey

7. PERFORMING ORGANIZATION NAME(S) AND ADDRESS(ES)
Program in Atmospheric and Oceanic Sciences
University of Colorado
Stadium 255
Boulder, CO 80309-0311

8. PERFORMING ORGANIZATION REPORT NUMBER

9. SPONSORING / MONITORING AGENCY NAME(S) AND ADDRESS(ES)
Air Force Office of Sponsored Research
801 N. Randolph St., Rm 732
Arlington, VA 22203-1977

10. SPONSORING / MONITORING AGENCY REPORT NUMBER
153-[redacted]0771

11. SUPPLEMENTARY NOTES

12a. DISTRIBUTION / AVAILABILITY STATEMENT

Approve for Public Release: Distribution Unlimited

12b. DISTRIBUTION CODE

13. ABSTRACT *(Maximum 200 words)*

The objectives of this work were to measure reactive chlorine (Cl, ClO, and Cl2O2) and carbon dioxide (CO2) and to examine the mechanisms of ozone loss in the plumes of various rockets as part of an ongoing investigation of the impacts of rocket emissions on stratospheric ozone. This work has demonstrated that ozone losses in rocket plumes proceed at rates that can be explained by 'standard' ozone loss chemistry involving the ClO radical - chemistry that is analogous to that occurring in the winter polar vortices. This work has also helped to identify an error in a key kinetic parameter. In combination with fast response measurements of Cl and ClO in the plume of STS-106, we have shown that calculations based on the revised rate constant for ClO+ClO, along with consideration of non-linear effects, can explain ozone loss rates within the uncertainties of the measurements.

20030513 067

14. SUBJECT TERMS
Rocket Plumes
Chlorine photochemistry
Ozone Loss

15. NUMBER OF PAGES
2

16. PRICE CODE

17. SECURITY CLASSIFICATION OF REPORT	18. SECURITY CLASSIFICATION OF THIS PAGE	19. SECURITY CLASSIFICATION OF ABSTRACT	20. LIMITATION OF ABSTRACT

Real-time Measurements of Reactive Chlorine and Carbon Dioxide in Rocket Plumes

Final Project Report

Darin W. Toohey
Program in Atmospheric and Oceanic Sciences
311-UCB
University of Colorado,
Boulder, CO 80309-0311
(303) 735-0002

Contract number F49620-99-1-0131

Objectives

The objectives of this work were to measure reactive chlorine (Cl, ClO, and Cl_2O_2) and carbon dioxide (CO_2) and to examine the mechanisms of ozone loss in the plumes of various rockets as part of an ongoing investigation of the impacts of rocket emissions on stratospheric ozone. Following a budget revision and change of priorities of the mission scientist during the RISO campaign, the project was rescoped to emphasize ultra-fast response measurements of Cl and ClO with ancillary measurements of CO_2 in rocket plumes, with some ambient sampling to support the NASA/NOAA ACCENT campaigns of 1999 and 2000.

Accomplishments/New Findings

At the close of this 3-year project, we successfully met all of the objectives outlined in the original proposal, having demonstrated that ozone losses in rocket plumes proceed at rates that can be explained by 'standard' ozone loss chemistry involving theClO radical - chemistry that is analogous to that occurring in the winter polar vortices. This work has also helped to identify an error in a key kinetic parameter (the rate constant for the ClO+ reaction ClO) as first reported by Ross et al. (2000). In combination with fast response measurements of Cl and ClO in the plume of STS-106, we have shown that this rate parameter, along with consideration of non-linear effects can explain ozone loss rates within the uncertainties of the measurements (unpublished results described in Year 4 Annual Progress Report).

An unexpected result from this effort was the discovery of volatile particles likely composed of HNO_3 and H_2O in the fresh plumes of several small rockets (Atlas IIAS and Athena II). These particles persisted long after the plume had diluted, indicating that our understanding of evaporative properties of binary (or ternary?) particles is lacking. These results have important implications for evolution of the plume, including visibility of plumes and chemistry both in the plumes and as they mix with background air. To date, these potential effects are not included in models of plume impacts.

These results are now presented in 5 publications that have appeared in the peer-reviewed literature, four of which have appeared in press and are attached to this file for brevity.

Personnel Supported

- Darin Toohey, Associate Professor and Principal Investigator (1 month summer salary)
- Mr. Brett Thornton, Graduate Research Assistant (part-time salary)
- Ms. Amelia Gates (travel support)

Publications resulting from this work (pdf files attached to this report)

M.N. Ross, D.W. Toohey, W.T. Rawlins, E.C. Richard, K.K. Kelly, A.F. Tuck, M.H. Proffitt, D.E. Hagen, A.R. Hopkins, P.D. Whitefield, J.R. Benbrook, and W.R. Sheldon, Observation of Stratospheric Ozone Depletion Associated With Delta II Rocket Emissions, Geophys. Res. Lett., 27, 2209-2212, 2000.

P.J. Popp, B.A. Ridley, L.M. Avallone, D.W. Toohey, R.S. Gao, J.A. Newman, M.J. Northway, J.C. Holocek, D.W. Fahey, J.G. Walega, F.E. Grahek, O. Schmid, J.C. Wilson, T.L. Thompson, K.K. Kelly, R.L. Herman, M.N. Ross, and P.F. Zittel, The Emission and Chemistry of Reactive Nitrogen Species in the Plume of an Athena II Solid-Fuel Rocket Motor, Geophys. Res. Lett., 29, 10.1029, 2002GL015197, 2002.

A.M. Gates, L.M. Avallone, D.W. Toohey, A.P. Rutter, P.D. Whitefield, D.E. Hagan, A.R. Hopkins, M.N. Ross, P.F. Zittel, T.L. Thompson, R.L. Herman, and R.R. Friedl, In situ Measurements of Carbon Dioxide, 0.37-4.0 mm Particles, and Water Vapor in the Stratospheric Plumes of Small Rockets, J. Geophys. Res., 108, 10.1029/2002JD002121, 2002.

M.Y. Danilin, P.J. Popp, R.L. Herman, M.K.W. Ko, M.N. Ross, C.E. Kolb, D.W. Fahey, L.M. Avallone, D.W. Toohey, B.A. Ridley, O. Schmid, J.C. Wilson, D.G. Baumgardner, R.R. Friedl, T.L. Thompson, and J.M. Reeves, Quantifying Uptake of HNO3 and H2O by Alumina Particles in Athena-II Rocket Plume, J. Geophys. Res., 108, 10.1029/2002JD2601, 2003.

O. Schmid, C.A. Brock, J.M. Reeves, M. Ross, L.M. Avallone, A.M. Gates, D.W. Toohey, C. Weidinmyer, and J.C. Wilson, Size-resolved Measurements of Particle Emission Indices in the Stratospheric Plume of a Solid-Fueled Rocket Motor, J. Geophys. Res., 108, 10.1029/2002JD2486, 2003 (in press).

Interactions/Transitions
None to report.

New Discoveries, inventions, or Patent Disclosures
None to report, except for the results presented above.

Honor/Awards
None to report.

JOURNAL OF GEOPHYSICAL RESEARCH, VOL. 107, NO. D22, 4649, doi:10.1029/2002JD002121, 2002

In situ measurements of carbon dioxide, 0.37–4.0 μm particles, and water vapor in the stratospheric plumes of small rockets

Amelia M. Gates,[1] Linnea M. Avallone,[1] Darin W. Toohey,[2] Andrew P. Rutter,[3] Philip D. Whitefield,[4] Donald E. Hagen,[5] A. Raymond Hopkins,[4,6] Martin N. Ross,[7] Paul F. Zittel,[7] Thomas L. Thompson,[8] Robert L. Herman,[9] and Randall R. Friedl[9]

Received 22 January 2002; revised 18 April 2002; accepted 19 April 2002; published 27 November 2002.

[1] Carbon dioxide (CO_2) and large particles (0.37–4.0 μm) were measured in the stratospheric plume wakes of three rockets, an Atlas IIAS, a Delta II, and an Athena II. The correlations between CO_2 mass and particle number densities in each plume are consistent with the unique combination of solid and liquid engine emissions of each rocket. Measured size distributions indicate a 1.1 μm mode with density of 2 g cm^{-3}, consistent with spherical alumina particles emitted by solid rocket motors. Disagreement between the measured size distributions and the mean sizes inferred from the known alumina and CO_2 emission indices and an observed increase in the particle number emission index with altitude are evidence for large particle oversampling effects and the presence of condensed volatile compounds within the particle population. Direct evidence for the latter is a persistent ~0.5–1 part per million (ppm) shortfall of water vapor relative to CO_2 measured in the plume of the Athena II rocket based on the expected H_2O/CO_2 emission ratio. Although pure ice particles would not persist at the conditions of the measurements, a more stable coating of HNO_3 (as either nitric acid trihydrate or as a liquid layer) could have reduced the sublimation rate of the underlying ice, thereby increasing the lifetimes of volatile particles within the plume. If confirmed, such a process would have important implications for the radiative and chemical properties of rocket plumes, including global ozone depletion associated with rocket launch activities. *INDEX TERMS:* 0305 Atmospheric Composition and Structure: Aerosols and particles (0345, 4801); 0394 Atmospheric Composition and Structure: Instruments and techniques; 0340 Atmospheric Composition and Structure: Middle atmosphere—composition and chemistry; *KEYWORDS:* carbon dioxide (CO_2), H_2O, ozone depletion, rocket plumes, emissions

Citation: Gates, A. M., et al., In situ measurements of carbon dioxide, 0.37–4.0 μm particles, and water vapor in the stratospheric plumes of small rockets, *J. Geophys. Res.*, *107*(D22), 4649, doi:10.1029/2002JD002121, 2002.

1. Introduction

[2] Rockets used in the space transportation industry emit a variety of exhaust products directly into the middle and upper atmosphere. The potential effects of these emissions on climate and stratospheric ozone abundances were first discussed during the 1975 Climate Impact Assessment Program [see *Hoshizaki*, 1975], and there has been subsequent progress in understanding the composition of rocket engine emissions and their impacts on the stratosphere. Various models of the global atmosphere are in broad agreement that present-day global-averaged ozone loss from rockets is a few hundredths of a percent, a small fraction of that believed to be due to all industrial activities [*World Meteorological Organization* (*WMO*), 1992]. However, the representation of rocket emissions by the models has focused primarily on the solid rocket motors (SRMs) while excluding liquid propellants [*Prather et al.*, 1990, *Jackman et al.*, 1998; *Danilin et al.*, 2001]. Furthermore, the models may not include all of the important interactions between the rocket emissions and natural stratospheric processes. Therefore, until models are validated by observations directly within the stratospheric plumes of rockets, their predictions of ozone losses should be considered as lower limits to those that could be expected.

[3] Based on model predictions of the stratospheric impacts of SRM emissions, in particular their small potential to deplete ozone relative to other human activities

[1]Laboratory for Atmospheric and Space Physics, University of Colorado at Boulder, Boulder, Colorado, USA.
[2]Program in Atmospheric and Oceanic Sciences, University of Colorado at Boulder, Boulder, Colorado, USA.
[3]Cloud and Aerosol Sciences Laboratory, University of Missouri-Rolla, Rolla, Missouri, USA.
[4]Department of Chemistry, University of Missouri-Rolla, Rolla, Missouri, USA.
[5]Department of Physics, University of Missouri-Rolla, Rolla, Missouri, USA.
[6]Deceased.
[7]Aerospace Corporation, Los Angeles, California, USA.
[8]NOAA Aeronomy Laboratory, Boulder, Colorado, USA.
[9]Jet Propulsion Laboratory, Pasadena, California, USA.

0148-0227/02/2002JD002121$09.00

[*WMO*, 1992], rocket engine emissions have remained unregulated [*United Nations Environment Programme*, 2001]. This status relies upon the validity of a number of assumptions, including (1) that global models accurately predict ozone losses due to SRM emissions, (2) that ozone losses from liquid propellants do not substantially exceed those from SRMs, and (3) that future rocket emissions remain comparable to those at present. The commercial space transportation industry has grown much faster than the economy as a whole in recent years and is projected to continue to do so. Meanwhile, new liquid propellant rockets are being developed. Therefore, the impact of rocket emissions on stratospheric ozone must be more carefully examined in order to continue to meet the evolving information needs of policy makers [*Ko et al.*, 1994].

[4] To date, efforts to model the global impacts of rockets have focused on the gas (HCl and Cl_2) and particulate (alumina, or Al_2O_3) emissions from SRMs that reduce stratospheric ozone by enhancing abundances of inorganic chlorine and increasing the reactive surface area of particles [*Prather et al.*, 1990, *Jackman et al.*, 1998; *Danilin et al.*, 2001]. Chlorine chemistry has been studied extensively in recent years in an effort to assess the impact of chlorofluorocarbons (CFCs), such that the regional and global influences of gaseous chlorine compounds emitted by SRMs are reasonably well understood. Consequently, there is general agreement as to the extent of global stratospheric ozone losses associated with the increases of inorganic chlorine abundances due to SRMs. In contrast, the global impact of particles emitted by SRMs is uncertain and may even be more significant than that due to the gaseous chlorine emissions [*Danilin et al.*, 2001].

[5] A variety of heterogeneous reactions have been proposed that promote conversion of reservoir forms of inorganic chlorine into ozone destroying forms on alumina particles, for example,

$$ClNO_3 + HCl \rightarrow Cl_2 + HNO_3, \quad (1)$$

$$ClNO_3 + H_2O \rightarrow HOCl + HNO_3, \quad (2)$$

$$HCl + HOCl \rightarrow Cl_2 + H_2O, \quad (3)$$

though the list is not exhaustive, and only reaction (1) has been studied in any detail in the laboratory [*Molina et al.*, 1997]. Recent modeling studies [*Jackman et al.*, 1998; *Danilin et al.*, 2001] have demonstrated that ozone loss is critically sensitive to the fraction of alumina mass contained in particles small enough (<0.4 μm) to have atmospheric residence times exceeding a few months. In these models, when the mass fraction of submicron particles accounts for more than a few percent of the total alumina mass, the predicted ozone losses associated with heterogeneous reactions on alumina exceed those due solely to the increase in chlorine abundances. Although size distributions of alumina particles emitted by rockets have been studied by various researchers [*Brady and Martin*, 1995; *Cofer et al.*, 1987; *Dao et al.*, 1997; *Beiting*, 1997; *Ross et al.*, 1999], there is no consensus on the relative mass fraction of the submicron portion of the size distribution. Reported values for these important particles have ranged from 0.01% to 95% of the mass of emitted alumina. Consequently, lacking a clear understanding of the alumina size distribution, the estimates of the impact of SRMs are highly uncertain.

[6] Additional uncertainty concerns the chemical nature of the alumina surface at stratospheric conditions. The reactivity of alumina particles depends on the nature of their surfaces, including the nature and availability of condensed materials. Limited laboratory studies of alumina reactivity in the presence of HCl and H_2O [*Molina et al.*, 1997; *Nelson et al.*, 2001] suggest that alumina will adsorb volatile compounds which then determine the kinetics of the various heterogeneous reactions. Such volatiles could be derived from the stratospheric background or from compounds emitted by the rocket itself. Because condensed phases are known to play critical roles in stratospheric chemistry, it is important to understand the nature of the interactions of volatile compounds with alumina particles.

[7] In this paper we report on the first simultaneous measurements of particles and CO_2 in the plume wakes of three rockets that employ different mixtures of solid and liquid propellants. Previous measurements of SRM alumina particles were limited by the lack of a conservative tracer of the rate of propellant consumption, which precluded validation of the observed particle size distributions. The absolute emission of CO_2 is well understood in solid and liquid propellant rocket engines, such that this species serves as an excellent tracer to understand the emissions of less well-understood rocket combustion products and their impacts [*Schulte and Schlager*, 1996]. We use calculations from an after-burning rocket plume flow field model to establish expected ratios of the deposition rates of various plume species to that of CO_2 [e.g., see *Zittel*, 1994; *Denison et al.*, 1994]. Previous measurements also were not able to distinguish between nonvolatile (alumina) and volatile (e.g., ice compounds) components of the plume particle population. Here we examine correlations between CO_2 and particles and between CO_2 and H_2O, as well as particle size distributions, to infer some of the characteristics of alumina in SRM plumes. We discuss some important implications that these characteristics could have for assessments of the impact of rocket emissions on stratospheric ozone.

2. Observations

[8] The Atmospheric Chemistry of Combustion Emissions Near the Tropopause (ACCENT) campaigns took place in April and September 1999, during which the NASA WB-57F high-altitude aircraft carried instruments to measure a wide variety of gas and aerosol species in rocket plume wakes. In this paper we limit our attention to measurements of CO_2, particles with diameters between 0.37 and 4.0 μm, water vapor, and ambient pressures and temperatures.

[9] Data were obtained in the plume wakes of Atlas IIAS, Delta II, and Athena II launch vehicles that use different combinations of solid and liquid (kerosene and liquid oxygen) propellant rocket engines, thereby producing different relative emissions of CO_2, H_2O, and alumina, as summarized in Table 1. Atlas IIAS plume data were obtained between 22.97 and 23.92 UT (solar zenith angles, or SZA, >87°) on April 12, 1999, following launch at 22.83 UT from Cape Canaveral, Florida (28°33′N, 80°18′W).

Table 1. Emission Mass Ratios Relative to CO_2

Rocket	Altitude, km	Al_2O_3, g/g CO_2	H_2O, g/g CO_2	HCl, g/g CO_2
Athena II	16–19	0.94	0.78	0.36
Atlas IIAS	19	0.17	0.47	0.06
Delta II	19	0.37	0.57	0.12
	11–13	0.55	0.65	0.24

Delta II plume data were obtained between 18.61 and 19.41 UT (SZA ~34°) following launch at 18.53 on April 15, 1999, from Vandenberg Air Force Base, CA (34° 48′N, 120°37′W). Athena II plume data were obtained between 18.43 and 18.98 UT (SZA ~42°) following launch from Vandenberg AFB at 18.35 UT on September 24, 1999. Similar to previous studies [*Ross et al.*, 1997, 2000], the WB-57F (airspeed ~180 m s^{-1}) flew though each plume wake a number of times with encounters ranging from 10–70 s in duration. In general, each encounter was flown through different portions of the plume wake, and we assume that gas and particle enhancements are due solely to rocket engines, rather than to engine exhaust from the WB-57F.

[10] The Atlas IIAS plume was encountered fourteen times near 19 km altitude, and the WB-57F aircrew reported excellent plume visibility for about 60 min until sunset; however, a complete set of measurements was obtained only during two encounters. The Delta II plume was encountered 12 times, the first occurring at an altitude of 19 km. After the first encounter, the plume was no longer visible to the WB-57F aircrew at this altitude and the aircraft descended to the 11–12 km region where the plume maintained visibility. At these lower altitudes the Delta II burns six SRMs along with the liquid-fueled core stage, a configuration that differs from that at 19 km, where only three SRMs burn with the core stage. The Athena II plume was encountered six times, the first five near 19 km. After about 20 min, the aircrew reported difficulty locating the plume, and the aircraft descended to 17 km for one last encounter before landing. Following a discussion of the nature of the observed particle-CO_2 and H_2O-CO_2 relationships, we offer an explanation for these high-altitude visibility issues. Important quantities for all of the plume encounters are summarized in Table 2.

3. Measurements

[11] CO_2 abundances were measured at 5 Hz by infrared absorption using a nondispersive infrared detector (Li-Cor, Model 6251, Lincoln, Nebraska) repackaged for the low-temperature (~195–220 K) and low-pressure (60–200 hPa) WB-57F aircraft environment. The instrument detects differences in concentrations between two cells held at the same temperature (~30–40°C) and pressure (~400 hPa). Under controlled laboratory conditions, this instrument detects changes in CO_2 mixing ratios of less than 0.1 ppm in less than 1 s. On an airborne platform, measuring with this sensitivity requires extremely precise pressure and temperature control. During flight a constant mixing ratio is maintained in one of the cells (the "reference") by flowing a CO_2 standard of known concentration near 365

Table 2. Details of Plume Encounters

	A Start, UT sec	B End, UT sec	C T, K	D P, hPa	E [M], 10^{18} cm^{-3}	F Theta, K	G Max CO_2, ppm	H Int CO_2, 10^{-8} g s cm^{-3}	I Int Part, cm^{-3} s	J Int Part Corr, cm^{-3} s	K AvgCorr, (J/H)	L CO_2/Part, 10^{-12} g
990412												
Atlas	84641	84693	201.5	79.0	2.84	418	12.0	6.14	6348	7615	1.20	8.06
	84973	85017	200.0	70.0	2.54	428	5.9	1.74	2700	2895	1.07	6.01
990415												
Delta	67017	67023	210.6	65.0	2.24	460	27.0	1.36	1684	2896	1.72	4.70
	67936	67944	212.1	191.0	6.53	341	12.0	3.08	2558	4261	1.67	7.23
	67947	67952	213.5	188.0	6.38	344	9.0	1.39	1243	1810	1.46	7.68
	68135	68148	214.0	203.0	6.82	338	9.0	2.61	2348	3763	1.60	6.94
	68145	68149	213.8	202.0	6.85	338	2.3	0.28	371	428	1.15	6.54
	68379	68387	214.5	199.0	6.73	340	8.8	2.09	2015	3091	1.53	6.76
	68389	68395	214.2	204.0	6.90	338	2.4	0.32	458	505	1.10	6.33
	68408	68411	213.8	206.0	6.99	336	1.6	0.14	185	188	1.02	7.43
	68523	68535	218.2	225.0	7.48	334	2.5	0.50	612	688	1.12	7.27
	68536	68549	217.5	221.0	7.37	335	4.0	1.04	1324	1430	1.08	7.27
	68550	68562	216.5	214.0	7.16	336	5.7	2.02	2210	2710	1.23	7.45
	68742	68750	212.1	194.0	6.63	339	7.6	2.06	1920	2635	1.37	7.82
	68752	68765	212.1	198.0	6.73	337	5.7	1.27	1396	1717	1.23	7.40
	68767	68787	213.1	204.0	6.93	336	6.7	2.00	2374	3045	1.28	6.57
	68956	68974	214.0	206.5	7.03	336	5.3	2.02	2385	2962	1.24	6.82
	69146	69158	212.5	193.5	7.03	335	8.5	2.08	2306	2942	1.28	7.07
	69166	69206	212.6	195.5	6.85	337	4.5	3.57	4155	4741	1.14	7.53
	69357	69369	213.6	205.0	6.95	337	6.1	1.45	1720	2234	1.30	6.49
	69591	69601	212.4	192.0	6.53	341	7.6	1.90	1841	2376	1.29	8.00
	69619	69652	212.7	201.0	6.83	335	6.8	4.28	5193	6352	1.22	6.74
	69807	69822	213.3	201.2	6.84	335	4.5	1.35	1731	2104	1.22	6.42
	69855	69860	212.6	192.5	6.58	340	3.5	0.53	602	683	1.13	7.76
990924												
Athena	66376	66384	208.1	70.0	2.44	445	8.5	0.40	1052	1610	1.53	2.45
	66728	66737	207.8	68.8	2.40	447	4.7	0.33	1916	2480	1.29	1.31
	67073	67080	207.2	66.5	2.33	450	3.8	0.20	1204	1627	1.35	1.22
	67363	67382	207.0	68.6	2.40	445	5.3	0.44	1975	2629	1.33	1.69
	67721	67746	206.9	65.9	2.30	451	4.3	0.53	2846	3759	1.32	1.40
	68311	68324	201.5	93.2	3.35	397	2.5	0.31	1219	1394	1.14	2.24

ppm at a rate of ~0.01 STP L min^{-1}. Ambient air is compressed to ~500 hPa with a modified one-stage Teflon-valve diaphragm pump (KNF Neuberger N-026), and a portion of this flow is passed through the second cell (the "sample") at a rate of ~0.4 STP L min^{-1} providing a refresh rate of about 1 s^{-1}.

[12] The absolute pressure in the reference cell and the pressure differential between the two cells are controlled with custom-built electronics modeled after a commercial controller (Model 1250, MKS Instruments, Andover, Mass.). The detector is packaged in a sealed vessel, into which the flow through the reference cell is drained such that the entire contents of the vessel are held at the same pressure. Over the typical duration of a plume encounter (tens of seconds) variations of temperature and pressure in the box and the two detector cells are negligible relative to electronic noise. Consequently, atmospheric variability and electronic noise dominate the variations in signal reported here.

[13] For simplicity, and to avoid undesirable shifts during plume encounters, the temperature of the instrument was not controlled; rather, it was allowed to reach a self-heated value of about 30°C. Extensive calibrations in flights not shown here demonstrated that the instrument response varies by less than 1% at a constant pressure, and is well described by the ideal gas law. For the data reported here the precision of the instrument was better than 1 ppm at >1 Hz response and was improved with each flight by attenuating various sources of electronic noise.

[14] The accuracy of the CO_2 measurements depends on that of the standards used to calibrate the instrument. For these flights, with emphasis on fast measurements of enhancements in narrow plumes, the standards were only characterized to a few ppm, such that absolute CO_2 abundances are accurate only to this level. Enhancements of CO_2 observed during plume encounters are accurate to the level of uncertainty of the response (or "span") of the detector, which we estimate to be better than ±5% at 2σ. Mixing ratios of ambient CO_2 varied between 365 and 370 ppm during these flights; in this paper we are concerned only with plume enhancements in CO_2 above ambient values. The accuracy of those enhancements is limited by the knowledge of CO_2 in the air around the plume wake, which is estimated from observations of CO_2 immediately before and after plume ingress and egress, respectively. Except where noted, the overall 2σ uncertainty of the plume enhancements of CO_2 is the larger of ±0.5 ppm or ±5%.

[15] Number and size distributions of particles with diameters in the range 0.37 to 4.0 μm were measured by laser particle counters (LPCs) (Met One Model 237B) repackaged for the WB-57F [*Ross et al.*, 1999]. This size range likely includes most of the mass of alumina emitted by the rocket, although there is no consensus on the relative mass in the submicron portion of the size distribution, as noted earlier. Soot particles produced by the kerosene fueled engines of the ATLAS IIAS and Delta II rockets are likely too small (~0.02–0.04 μm) to be detected. The sizes of particles measured in flight are determined relative to laboratory calibrations using polystyrene latex spheres. The residence time of sample air between the inlet and the LPC detector volume is about 1.5 s.

[16] For the Atlas IIAS and Delta II plume encounters, a single LPC measured the total particle population. For the Athena II plume, two LPCs were employed in series, one to measure total particles and the other to measure particles remaining after the airflow was heated to 198°C. Because water, HCl, and HNO_3 evaporate at much lower temperatures, the heated LPC channel is believed to represent SRM alumina and a small amount of aluminum chlorides, whereas the unheated LPC channel represents the total aerosol including volatile components that survive the transit between the instrument inlet and the first LPC.

[17] Enhancements of large particles within rocket plumes are typically several orders of magnitude larger than background concentrations, such that the particle measurements are highly precise. For these flights, number densities of large particles were obtained every 0.6 s, whereas size distributions were determined whenever counts from 5000 particles were accumulated. At high particle number densities, particle counters are subject to saturation and undercounting ('coincidence losses'). Detailed laboratory tests with the LPCs indicate that the correction is small (less than 10%) at densities below 150 cm^{-3}, but exceed 100% at particle densities of 400 cm^{-3} and larger. Although densities larger than 350 cm^{-3} were observed mainly during the earliest plume encounters, some correction was necessary for all of the data. For the results reported here, this correction was determined from data obtained in the plume of the Delta II rocket, as described later. The most significant uncertainties in the particle measurements are due to sampling effects, primarily inertial enhancements around the WB-57F airframe and instrument inlet and impaction losses in transfer lines.

[18] Water vapor measurements were obtained only on September 24, 1999, in the Athena II plume wake with the JPL Laser Hygrometer [*May*, 1998]. The instrument features a near-infrared, tunable diode laser (TDL) spectrometer and an open-path optical cell external to the aircraft, minimizing sampling issues such as wall losses or evaporation of volatile particles. The JPL Laser Hygrometer has a precision of 0.030 ppm for 1.4-s-averaged data, and an accuracy of ±5% at 19 km altitude [*Kley et al.*, 2000]. Pressures and temperatures were measured at the nose of the WB-57F using a Weston 7881 T Series vibrating cylinder with an accuracy of better than ±1 hPa, and a Rosemount thermistor with an accuracy of better than ±1 K.

[19] Because we are interested in the point-by-point correlation between CO_2 and the other measurements, the data sets must be appropriately averaged and aligned. The particle measurements are inherently faster than those of CO_2, and so a five-point running mean has been applied to the raw 5 Hz CO_2 data. To account for the longer residence time of air in the CO_2 sample lines compared to the particle and water instruments, the CO_2 data were shifted backward in time by a few seconds based on the simultaneous 5-Hz measurements of ClO (D. Toohey, unpublished data, 1999). The results are then merged back into a spreadsheet with a timebase of 0.6 s as determined by the particle measurements. Thus, it is important to note that for the particle-CO_2 correlations, two consecutive CO_2 data points are not entirely independent. For the H_2O-CO_2 comparisons, the data rates are comparable and the ordered pairs can be considered as independent measurements (that is, only every other CO_2 data point is included in the analysis because the water measurements are reported every 1.4 s).

4. Results

4.1. Correlation of CO_2 and Particles

[20] Time series of CO_2 and particle number densities observed during the sixth pass through the plume of the Delta II rocket are shown in Figure 1. As was typical for all the plume encounters for each of the rockets, the two quantities are highly correlated. The CO_2 signal does not respond as rapidly to small-scale features as does that from the particle instrument (e.g., the peak at 68770 s), as expected. Such a tight correlation indicates that the distinct exhaust plumes from the Delta II rocket (a single kerosene fueled engine surrounded by three SRMs) are well mixed by turbulent processes by the time of the WB-57F encounters.

[21] A scatterplot of CO_2 mass and particle number densities for the entire set of low-altitude Delta II plume observations is shown in Figure 2. The data are not ordered with respect to time, indicating that the relationship between CO_2 and particle number is conserved as the plume slowly expands and mixes with background air. The scatter in Figure 2 can be explained by small differences in the response times of the instruments and the lower precision of the CO_2 measurements.

[22] The main feature of Figure 2 is the nonlinearity of particle number densities with increasing CO_2. Laboratory tests of the LPC with sodium chloride particles found coincidence losses large enough to explain this nonlinearity. These tests, which are referenced to an independent particle counter, are somewhat uncertain at the highest particle densities observed in dense plume regions. Therefore, based on the correlation shown in Figure 2, we derive a third-order polynomial function that best reduces the nonlinearity.

$$P_c = P_o - 1.0 \times 10^{-4} P_o^2 + 5.0 \times 10^{-6} P_o^3, \quad (4)$$

where P_o and P_c are the uncorrected and corrected particle number densities. A similar order is sufficient to explain the curvature observed in the laboratory tests. Although not shown here, application of this empirical correction factor to the Atlas IIAS and Athena II plume data also markedly improves the linearity of those correlations. On this basis, we conclude that the correlation nonlinearity is an instrumental effect, rather than a property of the plumes, and that both the CO_2 and particle instruments behaved consistently on all three flights. The coincidence loss corrections derived using equation (4) increase the total number of particles observed in the Atlas IIAS, Delta II, and Athena II plumes by 16, 29, and 32%, respectively. The values of the average corrections for each plume encounter are summarized in Table 2.

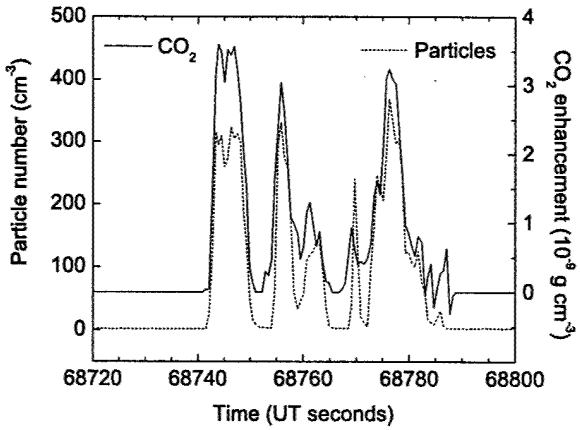

Figure 1. Traces of CO_2 mass density enhancements (solid line) and uncorrected large particle number densities (dashed line) in the plume of the Delta II rocket at ~11 km. The high degree of correlation on short timescales is typical of the measurements in other passes and for other rocket types.

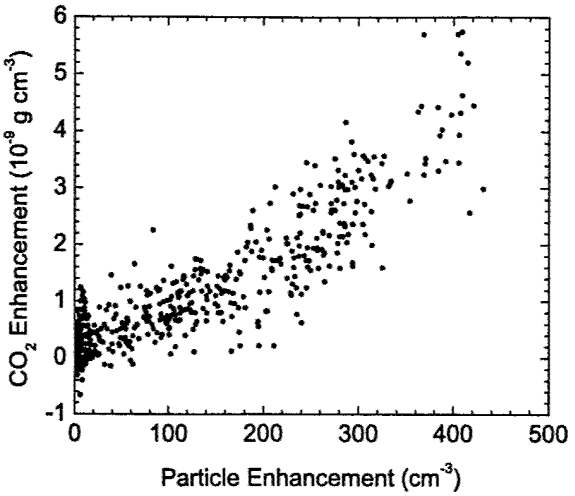

Figure 2. Scatterplot of enhancements of CO_2 versus enhancements of large particles for all of the low-altitude (~11–12 km) passes through the Delta II plume (67936-69860 s). Data from outside the plumes have been removed for clarity.

[23] Table 2 also presents the quantities of CO_2 mass and particle number densities integrated across each plume encounter. These integrated quantities are useful because they reduce random errors, eliminate scatter due to differences in instrument time response and data reporting times, and reduce the effects of incomplete mixing in the plumes. There is a high degree of consistency from encounter to encounter for each rocket, especially for the Delta II. Figure 3 shows the correlation between integrated mass of CO_2 and integrated number of particles for all the low-altitude plume encounters of the Delta II rocket. Although covering a large range in the magnitudes of these integrated quantities due to shearing and mixing processes, the results using corrected particle data fall on a line with a correlation coefficient of 0.99, whereas results based on the uncorrected particle data are significantly curved.

[24] CO_2 mass-to-particle number ratios integrated across each discreet plume segment are plotted in Figure 4 against the particle coincidence loss corrections averaged across each plume. There is a clear, systematic increase in these ratios with increasing average coincidence loss correction for the uncorrected particle number data, whereas the values using corrected particle number data are randomly scattered about an average of $\sim 7.2 \times 10^{-12}$ g CO_2 particle^{-1}. Further

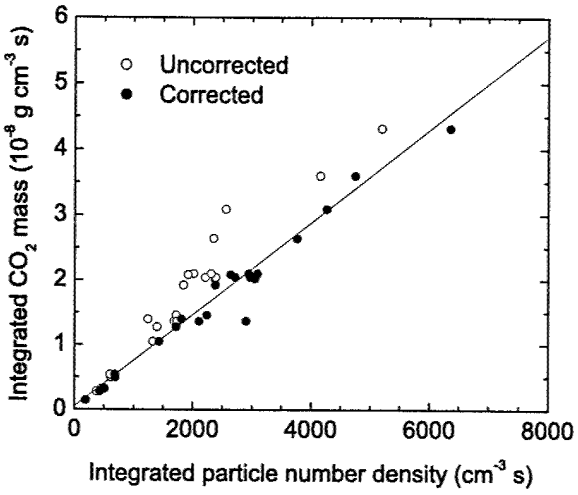

Figure 3. Correlation plot of CO_2 mass density enhancement versus particle number density enhancement, integrated across each discrete plume segment listed in Table 2 for the Delta II rocket. Open circles are determined from the "raw" particle number density measurements, whereas the solid circles represent those particle data that are corrected for coincidence losses. The outlier at integrated particle density ~3000 cm^{-3} is the first encounter at 19 km.

inspection of Table 2 reveals several trends in the data. First, for the measurements at lowest densities (19 km) there is a clear ordering of the CO_2/particle number ratio of about 7.5, 4.7, and 1.6 (10^{-12} g CO_2 particle^{-1}) (4.7 to 2.9 to 1) for the Atlas IIAS, Delta II, and Athena II, respectively. Assuming well mixed plume wakes at 19 km, the CO_2/alumina mass ratios for Atlas IIAS, Delta II, and Athena II are expected to be 5.9, 2.7, and 1.1 (5.4 to 2.5 to 1), respectively, similar to the observed ordering. This suggests

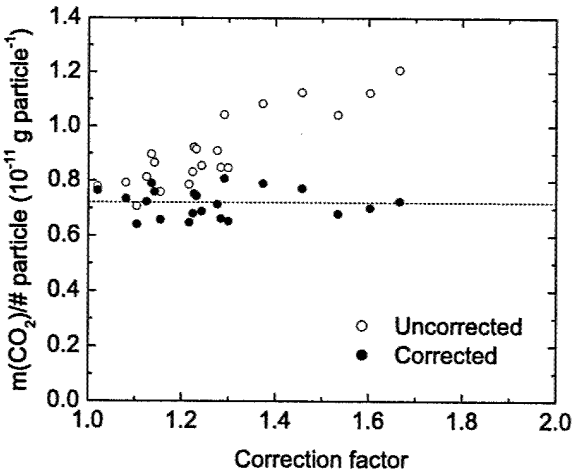

Figure 4. Scatterplot of the ratios of CO_2 mass-to-particle number for the low-altitude encounters with the Delta II plume as a function of the average coincidence loss correction. Symbols are as in Figure 3.

that the alumina particles emitted by the different SRMs used by the three rockets have similar physical characteristics (e.g., composition, diameter, and density).

[25] Second, the data show that CO_2 mass relative to the number of particles is correlated with altitude (or ambient pressure), whereas the ratio of the mass of CO_2 to mass of alumina is not expected to vary with altitude. With the exception of the first encounter of the Athena II plume, the data reveal a clear trend toward fewer particles, relative to CO_2, with decreasing altitude. This trend is most striking in the Delta II data, where the ratio of mass of CO_2 to mass of alumina is expected to be greater at 19 km than at 11–12 km, whereas the data present the opposite trend. Thus, assuming the particles have similar size distributions and densities, there are consistently more particles at high altitudes compared to low altitudes. Because we expect CO_2 to be a conservative tracer of propellant consumption, this trend must be the result of altitude-related variations in particle production mechanisms or in the detection efficiency of the LPCs. This conclusion is supported by detailed analysis of the Delta II plume particle size distributions presented below.

4.2. Particle Size Distributions

[26] The size distributions measured in each of the plumes are broadly consistent. Figure 5 shows the average of the differential number densities, dN/dD, versus particle diameter for each of the three rockets (after discarding the first encounter to minimize bias due to the relatively large coincidence loss corrections). To highlight differences in the shape of the distributions, we have normalized the results to the values at 0.91 μm. There is a mode of particles near 1.1 μm and, for the total LPC channel data, an increase in

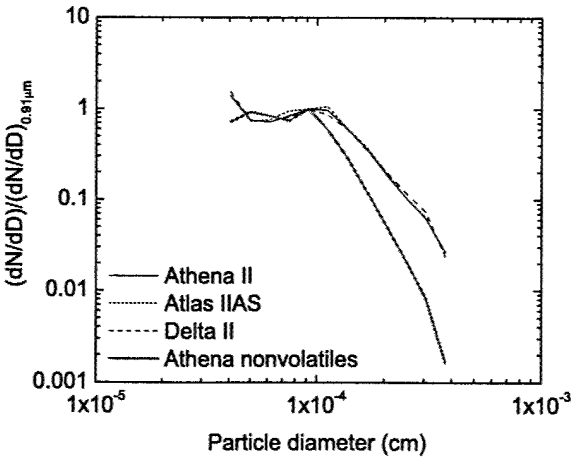

Figure 5. Average large-particle size distributions observed for each of the three rocket types (excluding the first pass through each of the three rockets where coincidence loss corrections were largest), normalized to the value at 0.91 μm. The total particle distributions from the three rockets are virtually indistinguishable, whereas the nonvolatile channel from the Athena II plume intercepts reveal a shift to smaller diameters and a relative "loss" of 0.37 μm particles.

differential number density at the smallest particle diameters detected by the LPC, suggestive of an additional mode outside of the LPC window. There is a hint of another, more variable, mode near 3 μm for all of the rockets, as reported in a previous study [*Cofer et al.*, 1987]. Otherwise, the distributions look remarkably similar.

[27] Focusing on the most extensive data set with the smallest potential sampling errors, the Delta II low altitude data, we determine the volume-averaged diameter from measured size distributions using the equation

$$\bar{D}(\mathrm{cm}) = \sqrt[3]{\frac{6\sum N(r)v(r)\delta(r)}{\pi\sum N(r)\delta(r)}}, \quad (5)$$

where v(r) is the volume of a sphere and N(r) is the size distribution measured in size bins of width δ(r). Gravitational settling and coagulation of particles smaller than 10 μm diameter are slow on the timescales of these measurements such that any changes in particle sizes must be due to condensation, evaporation, or evolution of particle density. A volume-weighted mean particle diameter of 1.5 μm is obtained if this average size distribution is extrapolated out to 6 μm assuming a lognormal distribution. This result is similar to those obtained in the plumes of large SRMs in the midtroposphere [*Cofer et al.*, 1987] and stratosphere [*Ross et al.*, 1999]. Based on the CO_2/particle ratios in Table 2 and the known CO_2-to-alumina mass ratio of 1.8 for the Delta II emission at 11–12 km, the particles would have a mean density of ~2 g cm^{-3}.

[28] There is considerable uncertainty regarding the density of alumina particles emitted by SRMs in the stratosphere [e.g., *Beiting*, 1997]. The value we derive is at the lower end of the range assumed by *Turco et al.* [1982] and reported by *Strand et al.* [1981], but nearly identical to the most likely value deduced by *Cofer et al.* [1987]. Because inertial enhancement effects would shift the apparent size distributions to larger sizes, and smaller particles may be composed of volatile materials (see below), the density determined from our measurements is likely a lower limit to the true value. Even so, we conclude that the particles are composed primarily of alumina and that the single 1.1 μm particle mode can account for all of the alumina emitted by the SRMs. Given the uncertainty in the effective alumina density, these data can not completely exclude some mass being in modes smaller than 0.3 μm. Because the density of alumina likely is not much smaller than 2 g cm^{-3}, we conclude that submicron particles probably do not contain more than a few tens-of-percents of the total mass of alumina emitted, eliminating the most extreme value that has been reported previously [*Dao et al.*, 1997].

[29] Assuming that the density of the particles observed at 19 km is also ~2 g cm^{-3}, the CO_2/particle ratios in Table 2 and the known emission indices imply a volume-weighted mean particle diameter of 1.1 μm for all three rockets. This value is somewhat smaller than that of 1.5 μm based on the size distributions shown in Figure 5. This difference can be explained in several ways. The mean density of alumina particles could be 60% smaller at 19 km than at 11–12 km, possibly because particle density varies inversely with size [*Beiting*, 1997] or is influenced by the presence of low density compounds. Alternatively, there could be a significant inertial enhancement of particles larger than 1 μm that increases with lower pressure and larger WB-57F airspeeds. Finally, the relative number of the smallest particles detectable by the LPC may be greater at 19 km than at lower altitudes. We discuss some important implications of these possibilities in the next section.

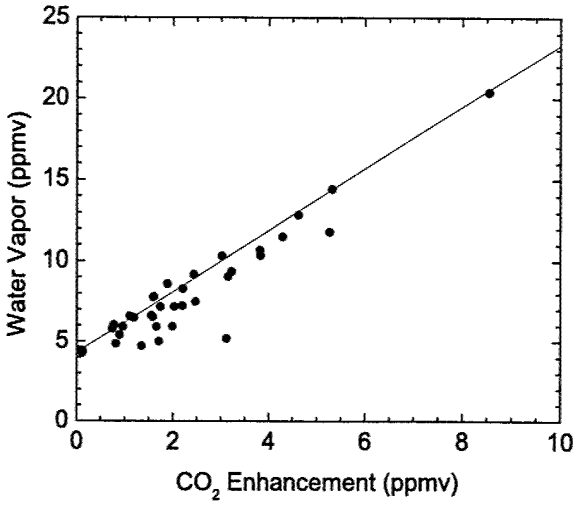

Figure 6. Scatterplot of observed total water vapor volume mixing ratios (in parts per million) versus CO_2 volume mixing ratio enhancements (in parts per million) for the first five passes through the plume of the Athena II rocket (66376–67746 s). Data outside of the plumes have been removed for clarity.

5. Discussion

[30] To first order, the particles emitted by the Atlas IIAS, Delta II, and Athena II rockets are characterized by a single mode of 1.1 μm with a density of about 2 g cm^{-3}, consistent with previous observations of alumina. In addition, at 19 km the comparative number of particles relative to CO_2 for each rocket is consistent with the trend in comparative emissions of alumina relative to CO_2 with rocket type (Table 1). Other aspects of the data require considerable elaboration to this overall picture, however. We showed above that the number of particles relative to CO_2 (i.e., the particle number emission index) tends to increase with decreasing ambient air density. It is reasonable to expect this to be due, at least in part, to nonrepresentative sampling of larger particles as a result of inertial enhancement effects that increase with altitude (e.g., lower ambient air densities and greater WB-57F airspeeds). Detailed characterization of the airflow around the WB-57F wing pod (where the LPC was located) and the airflow in the LPC inlet would be required in order to evaluate the magnitude of the inertial enhancements, which is beyond the scope of this study. Thus, we can only assume that some part of the data is explained by such an effect.

[31] There is a more intriguing explanation of the altitude variations of the particle characteristics. Volatile compounds condensed onto the alumina particles would modify their size and optical properties and, consequently, their ability to

be detected by the LPC. A variety of volatile compounds, such as H_2O, HCl, and HNO_3, are known constituents of SRM plumes. Based on measured CO_2 and the expected emission ratios, H_2O and HCl enhancements in the Athena II plume would be about 5–10 ppm and 1–2 ppm, respectively, and the relative humidity in some regions of the exhaust plume would likely exceed 100%. HNO_3 enhancements of 20–40 ppb were measured by *Neuman et al.* [2000] in the Athena II plume wake. With alumina serving as condensation nuclei, the conditions for volatile condensation are expected in the Athena II plume. Direct evidence for condensed volatile compounds is provided by measurements of water vapor mixing ratios in the Athena II plume, which are shown in Figure 6 as a function of CO_2 mixing ratios. Although highly correlated with CO_2, water vapor abundances exhibit a shortfall of about 0.5 to 1.5 ppm over the range of observed CO_2 enhancements compared to the expected H_2O to CO_2 molar emission ratio of 1.9. Condensation of this quantity of H_2O onto micron-sized alumina particles at typical plume number densities ($\sim 10^2$ cm^{-3}) would increase the apparent particulate volume by about one third. Alternatively, the same quantity of H_2O condensed onto 0.3 μm alumina particles could activate more than 500 cm^{-3} so that they would become detectable by the LPC, assuming they did not completely evaporate during the ~1.5 s transit from the inlet to the LPC detection volume.

[32] A comparison of the Athena II plume nonvolatile and total LPC size distributions in Figure 5 shows that the relative number of the smallest particles was indeed significantly reduced after the sample was heated, presumably due to evaporation of all water condensed on these particles. There was also a shift in apparent size toward larger particles for the total LPC distribution, which cannot be explained by condensation of only 1 ppm of water vapor. However, because the optical scattering properties of ice-coated alumina are significantly different from those of bare alumina, the LPCs could be overestimating the diameters of ice-containing particles. Whether the result of one or a combination of these effects, the water vapor shortfall and the different size distributions reported by the total and nonvolatile LPC channels provide strong evidence of condensed water in the Athena II plume.

[33] One difficulty with the conclusion that the Athena II particles contained significant quantities of volatile water is that pure ice is unstable at the temperatures and water vapor partial pressures in these plumes. Micron-sized pure ice particles produced in the plumes would have evaporated in $\sim 10^2$ s, before the WB-57F plume encounters [*Haynes et al.*, 1992]. However, H_2O equilibrium vapor pressures over admixtures of ice and nitric acid are significantly reduced [*Hanson and Mauersberger*, 1988] at the nitric acid partial pressures characteristic of the Athena II plume [*Neuman et al.*, 2000]. It is interesting to speculate how only 0.05 ppm of total HNO_3 could inhibit evaporation of nearly 1 ppm of condensed H_2O. An intriguing possibility is that the HNO_3 has combined with H_2O to form a few monolayers (e.g., $\sim 10^{15}$ molecules cm^{-2}) of a liquid or solid (e.g., nitric-acid trihydrate, or HNO_3*$3H_2O$). Such a coating on several hundred submicron particles would consume only a few ppb of gas-phase HNO_3. As argued previously [*Deshler et al.*, 1994, *Peter et al.*, 1994; *Livingston and George*, 1999; *Warshawsky et al.*, 1999], such a coating could significantly slow the evaporation of water trapped under the coating, possibly even preventing sublimation under conditions of ice subsaturation. Several modeling studies have found that the lifetimes of aircraft contrails may be extended similarly by uptake of HNO_3 into liquid aerosols (which may subsequently freeze) [*Gleitsmann and Zellner*, 1999] or onto surfaces of ice particles to form NAT [*Karcher*, 1996].

[34] Interestingly, based on the model of *Carslaw et al.* [1995] the evaporation points for solid HNO_3*$3H_2O$ (NAT) calculated using maximum water vapor mixing ratios determined from the CO_2 measurements and expected emission ratios (Table 1) were ~210 and ~213 K for the Delta II plume at 19 and 11–12 km, respectively, ~205 K for the Athena II plume (after the first pass), and ~207 K for the Atlas IIAS plume, assuming that maximum mixing ratios of HNO_3 were about 50 ppb. Ambient temperatures measured during the Atlas IIAS plume encounters, the majority of the Delta II low-altitude plume encounters, and the last encounter of the Athena II plume was at or below these threshold values, such that NAT (or a liquid HNO_3-H_2O mixture) were very likely present during these encounters. Even more interesting, the ambient temperatures measured during the 19 km passes through the Delta II and Athena II plumes were a few degrees above NAT threshold values. These were the intercepts for which the plumes were difficult to locate visually by the WB-57F aircrew. We note that submicron HNO_3*H_2O condensates would scatter visible light more efficiently than micron-sized alumina particles. Therefore, we propose that plume visibility may be linked to the presence of condensed mixtures of nitric acid and water, and that the persistence of condensed water ice in the Athena II plume may be the result of a thin coating of solid (i.e., NAT) or liquid HNO_3.

[35] Some condensed HCl might be expected in these volatile particles. The partitioning of chlorine in SRM plumes is time variable and complicated, as gas-phase and heterogeneous reactions such as reactions (1)–(3) convert it into active forms which react quickly with ambient ozone. Therefore, without time-resolved measurements of HCl it is difficult to speculate on its role in the condensed phase for these plumes. However, the same thermodynamic model [*Carslaw et al.*, 1995] suggests that it is likely that immediately after the plumes form (when HCl mixing ratios are a few ppm), significant quantities of this species would be in the condensed phase. Such partitioning would very likely accelerate heterogeneous conversion of $ClONO_2$ into HNO_3 via reactions (1) and (2), thereby providing a rapid source for the HNO_3 that would further stabilize ice particles formed in the expanding plume wake.

[36] Additional evidence for the presence of small volatile particles in rocket plumes is provided by multiwavelength Lidar observations of SRM plumes between 20 and 40 km [*Dentamaro et al.*, 1999]. The dependence of the plume backscatter with wavelength was found to evolve significantly within the first $\sim 10^3$ s after launch. Whereas the Rayleigh scattering dominated the Lidar signal shortly after launch, one hour later the signal was dominated by scattering from large particles. It was suggested that this may be due to the presence of evaporating aqueous HCl particles, but the rate of the observed changes was not consistent with that explanation [*Dentamaro et al.*, 1999]. Slowly evaporat-

ing nitric-acid coated particles can explain better the Lidar backscatter observations. It was further noted that similar behavior was not observed at 40 km, where nitric acid hydrates would not be stable. We conclude that small particles that contain condensed volatile materials likely play important roles in the plumes of most rockets.

6. Summary

[37] Data obtained in the plume wakes of Atlas IIAS, Delta II, and Athena II rockets using the WB-57F high-altitude aircraft shows that CO_2 mass and 0.37 to 4.0 μm particle number densities are highly correlated. The correlation is used to empirically correct the data for coincidence losses in the scattering volume of the laser particle counter and to deduce that the CO_2 and particle instruments performed consistently during the three flights. Constrained by measurements of CO_2 and the expected emission ratios for the three rockets, particle size distributions demonstrate that the mode of 1.1 μm particles with a density of 2 g cm^{-3} can account for all of the alumina mass emitted by the SRMs on these rockets. These data also suggest that submicron modes likely do not account for more than a few tens of percents of the total alumina mass.

[38] Using data obtained at 19 km under similar ambient conditions, we show that the observed differences in the relative abundances of CO_2 mass and particle number for different rockets are consistent with expected differences in the rocket emissions, assuming the particles are composed only of alumina. Several difficulties complicate the picture, however, and are difficult to explain. First, for constant rocket emission, the abundance of CO_2 relative to the number of particles decreases with altitude. Second, the particle size distributions contain more volume than can reasonably be accounted for by alumina alone. We propose that these are the result, in some combination, of inertial particle sampling effects and the presence of condensed water and nitric acid in the plumes.

[39] A correlation plot of water vapor and CO_2 in the Athena II plume wake reveals a shortfall, compared to the expected value, of about 0.5–1.0 ppm of water vapor under conditions of subsaturation with respect to pure ice, a shortfall that persists for more than 20 min. In conjunction with previously reported measurement of significant quantities of HNO_3 in the Athena II plume, we surmise that cocondensed nitric acid and water would likely have been stable in the conditions of the plume, and we note that there is more than enough nitric acid to coat the surfaces of the particles with many monolayers. We propose that such a coating limits the evaporation of water trapped in the particle (likely with an alumina core), thereby reducing the rate at which the particles evaporate in the atmosphere.

[40] If confirmed by future measurement and modeling efforts, the presence of volatile particles, admixtures of nitric acid and water in particular, in rocket plume wakes, would carry several significant implications. First, such particles are known to rapidly convert reservoir forms of chlorine into ozone-destroying forms, such as occurs in the polar lower stratosphere. Existing models of regional plume wake chemistry have not considered any of the variety of heterogeneous reactions that would proceed on volatile surfaces, and such reactions may contribute to the observed fast removal of ozone in rocket plume wakes. Even more troublesome, the lifetimes of such particles, which have not been considered in model studies of rocket impacts, may be quite long in the winter polar stratosphere where conditions remain close to NAT saturation for several months. Consequently, high-latitude rocket launches into the polar vortex could have important implications for polar ozone loss.

[41] Our results also suggest that some combinations of rocket engines may be more harmful to stratospheric ozone than others. Some launch vehicles combine SRMs (emitting H_2O and alumina particles) and an engine using N_2O_4 and hydrazine compounds. The NO_x emission index for hydrazine fueled rocket engines is predicted to be at least twenty times that for SRMs in the stratosphere (unpublished combustion models). In the plume wakes of such vehicles, the additional NO_x would rapidly form additional HNO_3 so that this combination of rocket engines could be a much more prodigious source of NAT particles than either engine alone. Finally, our results emphasize the significant gaps in knowledge regarding rocket emissions and their impact on ozone, particularly regarding particles, liquid rocket emissions, and the unique interactions of the different emissions used by the various launch vehicles around the world.

[42] **Acknowledgments.** We thank the ground and flight crews of the NASA WB-57F aircraft for their efforts in making these studies possible. In particular, we appreciate the help of Bud Meins, Gary Ash, and Shelley Hilden with instrument integration. Hiro Kosai, Zach Castleman, and Dylan Yaney helped to design and build instrument electronics and mounting hardware. Brett Thornton provided assistance in the field. A.M.G. acknowledges support from a NASA Earth System Science Fellowship. L.M.A. acknowledges support for instrument development from the NASA Atmospheric Effects of Aviation Program, under the direction of Don Anderson. D.W.T. received support from the Air Force Office of Sponsored Research, under the direction of Mike Berman, and travel support from the NASA AEAP.

References

Beiting, E. J., Solid rocket motor exhaust model for alumina particles in the stratosphere, *J. Spacecr. Rockets*, *34*, 303–310, 1997.

Brady, B. B., and L. R. Martin, Modeling solid rocket booster exhaust plumes in the stratosphere with SURFACE CHEMKIN, *TR-95(5231)-9, SMC-TR-96-19*, Aerospace Corp., El Segundo, Calif., 1 September 1995.

Carslaw, K. S., S. L. Clegg, and P. Brimblecombe, A thermodynamic model of the system HCl - HNO_3 - H_2SO_4 - H_2O, including solubilities of HBr, from <200 K to 328 K, *J. Phys. Chem.*, *99*, 11,557–11,574, 1995.

Cofer, W. R., III, G. G. Lala, and J. P. Wightman, Analysis of mid-tropospheric space shuttle exhausted aluminum oxide particles, *Atmos. Environ.*, *21*, 1187–1196, 1987.

Danilin, M. Y., R. L. Shia, M. K. W. Ko, D. K. Weisenstein, N. D. Sze, J. J. Lamb, T. W. Smith, P. D. Lohn, and M. J. Prather, Global stratospheric effects of the alumina emissions by solid-fueled rocket motors, *J. Geophys. Res.*, *106*, 12,727–12,738, 2001.

Dao, P. D., J. A. Gelbwachs, R. Farely, R. Garner, P. Soletsky, and G. Davison, Stratospheric SRM exhaust plume measurements, paper presented at 35th Aerospace Science Meeting, Am. Inst. of Aeronaut. and Astronaut., New York, 1997.

Denison, M. R., J. J. Lamb, W. D. Bjorndahl, E. Y. Wong, and P. D. Lohn, Solid rocket exhaust in the stratosphere: Plume diffusion and chemical reactions, *J. Spacecr. Rockets*, *31*, 435–442, 1994.

Dentamaro, A. V., P. D. Dao, R. Farley, and M. Ross, Characterization of particles from stratospheric launch vehicle plumes using wavelength-dependent Lidar techniques, *Geophys. Res. Lett.*, *26*, 2395–2398, 1999.

Deshler, T., T. Peter, R. Müller, and P. Crutzen, The lifetime of leewave-induced ice particles in the Arctic stratosphere, I, Balloon-borne measurements, *Geophys. Res. Lett.*, *21*, 1327–1330, 1994.

Gleitsmann, G., and R. Zellner, The aerosol dynamics of H_2O-H_2SO_4-HNO_3 mixtures in aircraft wakes: A modeling study, *Phys. Chem. Chem. Phys.*, *1*, 5503–5509, 1999.

Hanson, D. R., and K. Mauersberger, Laboratory studies of the nitric acid

trihydrate: Implications for the South Polar stratosphere, *Geophys. Res. Lett.*, *15*, 855–858, 1988.

Haynes, D. R., N. J. Tro, and S. M. George, Condensation and evaporation of H_2O on ice surfaces, *J. Phys. Chem.*, *96*, 8502–8509, 1992.

Hoshizaki, H., Aircraft wake microscale phenomena, in *The Stratosphere Perturbed by Propulsion Effluents, CIAP Monogr. Ser.*, vol. 3, chap. 2, pp. 60–73, Clim. Impact Assess. Program, U.S. Dep. of Transp., Washington, D.C., September 1975.

Jackman, C. H., D. B. Considine, and E. L. Fleming, A global modeling study of solid rocket aluminum oxide emission effects on stratospheric ozone, *Geophys. Res. Lett.*, *25*, 907–910, 1998.

Karcher, B., Aircraft-generated aerosols and visible contrails, *Geophys. Res. Lett.*, *23*, 1933–1936, 1996.

Kley, D., J. W. Russell III, and C. Phillips, SPARC Assessment of Upper Tropospheric and Stratospheric Water Vapour, *WCRP-113, WMO/TD 1043, SPARC Rep. 2*, World Meteorol. Org., Geneva, 2000.

Ko, M. K. W., N. Sze, and M. J. Prather, Better protection of the ozone layer, *Nature*, *367*, 505–508, 1994.

Livingston, F. E., and S. M. George, Effect of HNO_3 and HCl on HDO diffusion on crystalline D_2O ice multilayers, *J. Phys. Chem. B*, *103*, 4366–4376, 1999.

May, R. D., Open-path, near-IR tunable diode laser spectrometer for atmospheric measurements of H_2O, *J. Geophys. Res.*, *103*, 19,161–19,172, 1998.

Molina, M. J., L. T. Molina, R. Y. Zhang, R. F. Meads, and D. D. Spencer, The reaction of $ClONO_2$ with HCl on aluminum oxide, *Geophys. Res. Lett.*, *24*, 1619–1622, 1997.

Nelson, C. E., J. W. Elam, M. A. Tolbert, and S. M. George, H_2O and HCl adsorption on single crystal α-Al_2O_3 (0001) at stratospheric temperatures, *Appl. Surf. Sci.*, *171*, 21–33, 2001.

Neuman, J. A., et al., A fast-response chemical ionization mass spectrometer for in situ measurements of HNO_3 in the upper troposphere and lower stratosphere, *Rev. Sci. Instrum.*, *71*, 3886–3894, 2000.

Peter, T., R. Müller, P. Crutzen, and T. Deshler, The lifetime of lee-wave-induced ice particles in the Arctic stratosphere, II, Stabilization due to NAT coating, *Geophys. Res. Lett.*, *21*, 1331–1334, 1994.

Prather, M. J., M. M. García, A. R. Douglass, C. H. Jackman, M. K. W. Ko, and N. D. Sze, The space shuttle's impact on the stratosphere, *J. Geophys. Res.*, *95*, 18,583–18,590, 1990.

Ross, M. N., J. O. Ballenthin, R. B. Gosselin, R. F. Meads, P. F. Zittel, J. R. Benbrook, and W. R. Sheldon, In-situ measurements of Cl_2 and O_3 in a stratospheric solid rocket motor exhaust plume, *Geophys. Res. Lett.*, *24*, 1755–1758, 1997.

Ross, M. N., P. D. Whitefield, D. E. Hagen, and A. R. Hopkins, In situ measurement of the aerosol size distribution in stratospheric solid rocket motor exhaust plumes, *Geophys. Res. Lett.*, *26*, 819–822, 1999.

Ross, M. N., et al., Observation of stratospheric ozone depletion associated with Delta II rocket emissions, *Geophys. Res. Lett.*, *27*, 2209–2212, 2000.

Schulte, P., and H. Schlager, In-flight measurements of cruise altitude nitric oxide emission indices of commercial jet aircraft, *Geophys. Res. Lett.*, *23*, 165–168, 1996.

Strand, L. D., J. M. Bowyer, G. Varsi, E. G. Laue, and R. Gauldin, Characterization of particulates in the exhaust plume of large solid-propellant rockets, *J. Spacecr. Rockets*, *18*, 297–305, 1981.

Turco, R. P., O. B. Toon, and R. C. Whitten, Space-shuttle ice nuclei, *Nature*, *298*, 830–832, 1982.

United Nations Environment Programme, Report of the Thirteenth Meeting of the Parties to the Montreal Protocol on Substances that Deplete the Ozone Layer, *Rep. OzL. Pro. 13/10*, Nairobi, 26 October 2001.

Warshawsky, M. S., M. A. Zondlo, and M. A. Tolbert, Impact of nitric acid on ice evaporation rates, *Geophys. Res. Lett.*, *26*, 823–826, 1999.

World Meteorological Organization, Scientific Assessment of Ozone Depletion: 1991, *WMO Rep. 37*, Geneva, 1992.

Zittel, P. F., Computer model predictions of the local effects of large, solid-fuel rocket motors on stratospheric ozone, *Rep. TR-94(4231)-9*, Aerospace Corporation, El Segundo, Calif., 1994.

L. M. Avallone and A. M. Gates, Laboratory for Atmospheric and Space Physics, University of Colorado at Boulder, 590 UCB, Boulder, CO 80309-0590, USA. (avallone@lasp.colorado.edu; amelia.gates@colorado.edu)

R. R. Friedl and R. L. Herman, Jet Propulsion Laboratory, MS 183-401, 4800 Oak Grove Drive, Pasadena, CA 91109, USA. (randall.r.friedl@jpl.nasa.gov; robert.l.herman@jpl.nasa.gov)

D. E. Hagen, Department of Physics, University of Missouri-Rolla, 1870 Miner Circle, G11 Norwood, Rolla, MO 65409, USA. (hagen@umr.edu)

M. N. Ross and P. F. Zittel, Aerospace Corporation, PO Box 92957, Los Angeles, CA 90009-2957, USA. (martin.n.ross@aero.org; paul.f.zittel@aero.org)

A. P. Rutter, Cloud and Aerosol Sciences Laboratory, University of Missouri-Rolla, 1870 Miner Circle, G7 Norwood, Rolla, MO 65409, USA. (arutter@umr.edu)

T. L. Thompson, NOAA Aeronomy Laboratory, R/E/AL, 325 Broadway, Boulder, CO 80305, USA. (thomas.l.thompson@al.noaa.gov)

D. W. Toohey, Program in Atmospheric and Oceanic Sciences, University of Colorado at Boulder, 311 UCB, Boulder, CO 80309-0311, USA. (toohey@colorado.edu)

P. D. Whitefield, Department of Chemistry, University of Missouri-Rolla, 1870 Miner Circle, G11 Norwood, Rolla, MO 65409, USA. (pwhite@umr.edu)

JOURNAL OF GEOPHYSICAL RESEARCH, VOL. 108, NO. D4, 4141, doi:10.1029/2002JD002601, 2003

Quantifying uptake of HNO_3 and H_2O by alumina particles in Athena-2 rocket plume

M. Y. Danilin,[1] P. J. Popp,[2,3] R. L. Herman,[4] M. K. W. Ko,[5,6] M. N. Ross,[7] C. E. Kolb,[8] D. W. Fahey,[2,3] L. M. Avallone,[9] D. W. Toohey,[9] B. A. Ridley,[10] O. Schmid,[11,12] J. C. Wilson,[11] D. G. Baumgardner,[13] R. R. Friedl,[4] T. L. Thompson,[2] and J. M. Reeves[11]

Received 31 May 2002; revised 16 August 2002; accepted 19 August 2002; published 27 February 2003.

[1] The goal of this study is to quantify uptake of H_2O and HNO_3 by and estimate their residence time on alumina particles in Athena-2 rocket plumes. This study uses in situ measurements made in the lower stratosphere with the NASA WB-57F high-altitude aircraft on 24 September 1999. Constraining the Atmospheric and Environmental Research, Inc. (AER), plume model with available measurements, we found that (1) H_2O uptake coefficient for alumina particles is larger than 3×10^{-4}, (2) HNO_3 is produced via $ClONO_2 + HCl \rightarrow Cl_2 + HNO_3$ on alumina particles and resides on their surfaces for 5–52 min, and (3) alumina particles in the plume are covered by 100–200 monolayers of adsorbed H_2O and 0.1–10 monolayers of HNO_3 under lower stratospheric conditions. These values are uncertain by at least a factor of 2. We speculate that the H_2O coverage remaining on alumina particles accelerates the $ClONO_2 + HCl \rightarrow Cl_2 + HNO_3$ reaction, thus leading to a larger than previously thought global ozone loss to solid-fueled rocket emissions, especially if at least several percent of emitted alumina mass are in submicron particles. *INDEX TERMS:* 0305 Atmospheric Composition and Structure: Aerosols and particles (0345, 4801); 0317 Atmospheric Composition and Structure: Chemical kinetic and photochemical properties; 0340 Atmospheric Composition and Structure: Middle atmosphere—composition and chemistry; *KEYWORDS:* alumina particles, uptake of HNO_3 and H_2O, rocket emissions

Citation: Danilin, M. Y., et al., Quantifying uptake of HNO_3 and H_2O by alumina particles in Athena-2 rocket plume, *J. Geophys. Res.*, *108*(D4), 4141, doi:10.1029/2002JD002601, 2003.

1. Introduction

[2] Launches of solid-fueled rockets cause a particular concern primarily because of emissions of chlorine and alumina particles directly into the stratosphere, thus depleting the ozone layer [*Prather et al.*, 1990; *Ko et al.*, 1994; *Jackman et al. 1998*; *World Meteorological Organization* (*WMO*), 1992]. Recent analysis of solid-fueled rocket plumes shows almost complete depletion of ozone locally [e.g., *Ross et al.*, 2000], however, global implications of such sharp local ozone reductions are predicted to be small [*Danilin et al.*, 2001a]. On the other hand, the heterogeneous reaction (R1) on alumina particles:

$$\text{(R1)} \qquad ClONO_2 + HCl \xrightarrow{Al_2O_3} Cl_2 + HNO_3$$

with the reaction probability of $\gamma = 0.02$ [*Molina et al.*, 1997] does not play an important role in local ozone depletion [*Danilin et al.*, 2001a]. However, it becomes important on the global scale by converting emitted and, more importantly, background HCl into short-lived Cl_2 resulting in ozone depletion that would correspond to an ozone depletion potential (ODP) of alumina particles larger than 0.2 depending on the location of emissions, size distribution of alumina particles, and the value of (R1) reaction probability [*Danilin et al.*, 2001b]. Since the (R1) rate is quite different for pure [*Molina et al.*, 1997] and covered by H_2O [*Shi et al.*, 2001] alumina, we try to quantify the uptake of H_2O and HNO_3 by rocket plume alumina particles using relevant measurements obtained during the Atmospheric Chemistry of Combustion Emissions Near the Tropopause (ACCENT) campaign. This mission sponsored by NASA and the US Air Force took place in 1999–2000 and was designed to investigate the impact of rocket and aircraft emissions near the tropopause.

[1]The Boeing Company, Seattle, Washington, USA.
[2]Aeronomy Laboratory, NOAA, Boulder, Colorado, USA.
[3]Cooperative Institute for Research in Environmental Sciences, University of Colorado, Boulder, Colorado, USA.
[4]Jet Propulsion Laboratory, Pasadena, California, USA.
[5]Atmospheric and Environmental Research, Inc., Lexington, Massachusetts, USA.
[6]Now at NASA Langley Research Center, Hampton, Virginia, USA.
[7]The Aerospace Corporation, Los Angeles, California, USA.
[8]Aerodyne Research, Inc., Billerica, Massachusetts, USA.
[9]University of Colorado, Boulder, Colorado, USA.
[10]National Center for Atmospheric Research, Boulder, Colorado, USA.
[11]University of Denver, Denver, Colorado, USA.
[12]Now at Max Plank Institute for Chemistry, Mainz, Germay.
[13]National University of Mexico, Mexico City, Mexico.

0148-0227/03/2002JD002601S09.00

2. Results and Discussion

2.1. Measurements

[3] During the ACCENT campaign, emissions of four different rockets were sampled by the NASA WB-57F aircraft. We focused our study on the 24 September 1999 flight because the NOAA chemical ionization mass spectrometer (CIMS) and JPL laser hygrometer made simultaneous measurements of HNO_3 and H_2O, respectively, in a rocket plume during this flight only. An Athena-2 was launched at 11.21 am PST on 24 September 1999 from Vandenberg Air Force Base in California. Figure 1 shows the location of the Athena-2 plume measurements. The WB-57F aircraft made six intercepts of the rocket plume with the first five samplings occurring near 70 hPa (~18.6 km) and the last intercept at 97 hPa (~16 km). Plume ages ranged from 3.7 to 36.2 min (see Table 1). The burning of 1 kg of Athena-2 solid rocket fuel resulted in 1.27 kg of exhaust with emission indices (EI) for the main products of 382, 300, 362, 217, and 2 g/kg(fuel) for CO_2, H_2O, alumina, chlorine (as HCl), and NO, respectively. In this study the following measurements are used: CO_2 [*Gates et al.*, 2002], H_2O [*May*, 1998], NO_y, HNO_3, [*Popp et al.*, 2002], and particles [*Schmid et al.*, 2002; *Baumgardner et al.*, 1996]. Perturbations of relevant species and Al_2O_3 particles in these plumes are given by *Popp et al.* [2002] and *Schmid et al.* [2002]. *Fahey et al.* [1995] showed that it is better to use plume-averaged values for a quantitative analysis, since different instruments have different sampling rate and plume composition is inhomogeneous. Below, we follow this methodology for comparison of plume-averaged values for each interception against our model calculations. Previous studies [*Popp et al.*, 2002; *Herman et al.*, 2001; *Gates et al.*, 2002] revealed that nitric acid and water vapor must have condensed on particles in the Athena-2 plumes in order to explain their measurements. This finding is surprising, since for the reasonable plume dilution scenarios and ambient temperature of 208.1 and 200.2 K at 70 and 97 hPa, respectively, H_2O and HNO_3 were not saturated with respect to ice or nitric acid trihydrate (NAT). Our paper extends their analysis by proposing mechanisms of the HNO_3 and H_2O condensation onto alumina particles under those conditions and discusses implications of the results.

2.2. Model

[4] In order to address this issue, we apply the Atmospheric and Environmental Research, Inc. (AER), plume model [*Danilin et al.*, 2001a], which was initialized by the Aerospace model output (P. F. Zittel, personal communication, 2001) for the Athena-2 emissions along its 24 September 1999 trajectory with the fuel consumption rate of 14 and 15 g per vertical cm at 18.6 and 16 km, respectively. The plume dilution rate was constrained by the CO_2 measurements, since carbon dioxide is chemically inert and its emission index is well-known (EI(CO_2) = 382 g/kg(fuel)). Since plume composition is spatially inhomogeneous and the distance from the plume centerline for each interception is unknown, we treat each plume event indi, vidually in our model. The model assumes a homogeneous distribution of species in the plume. Since we study linear processes here (such as uptake of HNO_3 and H_2O which is linearly proportional to Al_2O_3 SAD), it is reasonable to compare model results against plume-averaged measurements. Varying the initial plume cross section and its dilution rate, we match the plume width and CO_2 concentration at the time of measurements (see Figure 2a). Since the shape of the plume sampled by the aircraft is unknown, for simplicity we assume that the plume is circular with diameters known from the measurements. This assumption may introduce additional uncertainty in our analysis. Mixing with ambient air was parameterized as given by *Danilin et al.* [2001a] and the values of ambient species used are the WB-57F measurements just outside the plumes.

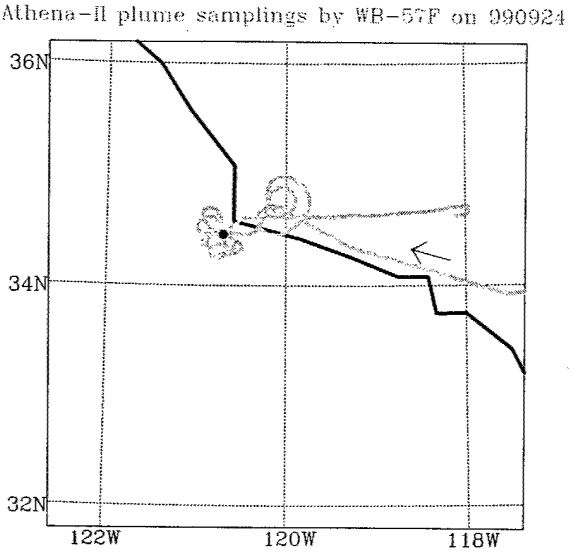

Figure 1. Location of the Athena-2 plume measurements (red dot) and the WB-57F aircraft flight track (green line) near California coast on 24 September 1999.

[5] Our model starts calculations 5 s after exhaust when plume temperature approaches its ambient values and standard photochemical kinetics [*Sander et al.*, 2000] is applicable. In this approach, we overlook important microphysical processes (like possible rapid H_2O condensation onto and its evaporation from alumina particles [*Gates et al.*, 2002]) in the near-field. To address this issue, model sensitivity studies were made (see section 2.5).

[6] The alumina particles in the plumes are treated as non-interactive spheres in 40 bins with diameters ranging from 0.78 nm to 6.4 μm. The shape of the Al_2O_3 size distribution is obtained by combining aerosol instrument measurements by the nucleation-mode aerosol mass spectrometer (NMASS) and focused cavity aerosol spectrometer (FCAS) instruments [*Schmid et al.*, 2002] for $d \leq 1.1$ μm and from Multiple-Angle Aerosol Spectrometer Probe (MASP) data [*Baumgardner et al.*, 1996] for particles with $d > 1.1$ μm, thus covering the range from 4 nm to 20 micron. Their initial distribution in our model is normalized in order to be consistent with the measurements at the time of plume intercepts (see Figure 2c). Omission of possible coagulation of alumina particles is not important, since it does not affect micron-size particles (which determine the alumina surface area density (SAD) and thus are the most

Table 1. Age and Diameters of Plume Sampled and Plume-Averaged Measured and Calculated Values of Water and Nitric Acid[a]

			H_2O, ppmv				HNO_3, ppbv						
Plume	Age, min	D, km	Meas[b]	Model	Con	α_2	Meas[c]	Gas[d]	Con[d]	$\tau_1^{\alpha_1=0}$	$\tau_1^{\alpha_1=1}$	EI, g/kg	SAD, $\mu m^2/cm^3$
1	3.7	1.21	10.26	11.62	1.36	12.5	25.6	3.0	3.5	-	103	4.0	-
2	9.7	1.95	7.68	8.08	0.40	6.2	19.4	3.0	2.5	52	15	3.2	892
3	15.4	1.15	7.23	7.97	0.74	5.7	19.7	4.9	2.5	17	6	2.7	831
4	20.3	2.71	6.90	7.78	0.88	5.3	12.8	2.6	1.5	22	5	2.0	461
5	26.3	2.59	7.51	8.45	0.94	3.4	19.8	4.3	2.6	31	7	2.2	935
6	36.2	1.91	8.07	8.76	0.69	2.7	15.5	3.0	2.2	30	9	2.0	526

[a]D, diameter; Meas, measured values; and Model, calculated values. The columns (con) show the amount of condensed H_2O and HNO_3 together with the required uptake coefficient α ($\times 10^{-4}$) of H_2O and residence time (τ_1, in min) of HNO_3 on alumina Sites. Derived EI(NO_2) and measured Al_2O_3 SAD are also listed.
[b]Gas-phase only.
[c]Gas and condensed.
[d]$\alpha_1 = 0$.

important in the context of this study) during the first hour after exhaust.

[7] Since the rocket near-field model calculations of NO are quite uncertain (P. F. Zittel, personal communication, 2001), we chose initial concentration of NO in a such way that model NO_y is consistent with the measured NO_y at the time of plume intercepts (see Figure 2b). Following this approach, we obtained EI(NO) shown in Table 1 and expressed in g(NO_2)/kg(fuel). Our EI(NO) values are in good agreement with those reported by *Popp et al.* [2002], who used a different approach analyzing the plume averaged values of CO_2 and NO_y in order to derive EI(NO). The rocket combustion models predict that the initial partitioning of chlorine between Cl_2 and HCl should be 35% and 65% by mass, respectively [*Zittel*, 1994]. In our calculations we used ozone measurements [*Richard et al.*, 2001] in order to determine this partitioning for each plume intercept. The derived Cl_2 fraction varied between 5 and 15%. Below we discuss uncertainties related to the initial chlorine partitioning.

2.3. HNO_3

[8] Nitric acid may appear on alumina particles via both heterogeneous reactions and kinetic uptake after collisions and leave via desorption. Thus, the temporal evolution of HNO_3 condensed onto particles ignoring plume dilution is described by

$$\frac{dHNO_3^c}{dt} = \frac{SAD\left(\gamma v ClONO_2^g + \alpha_1 v_1 HNO_3^g\right)}{4} - \frac{HNO_3^c}{\tau_1}. \quad (1)$$

Here SAD is the surface area density of Al_2O_3 particles, γ = 0.02 [*Molina et al.*, 1997], α_1 is the uptake coefficient, v and v_1 are the mean thermal speeds of $ClONO_2$ and HNO_3 molecules, respectively, τ_1 is the residence time of HNO_3 on alumina surface, superscripts g and c mean gas and condensed phases, respectively. Since the OH mixing ratio is about 0.01–0.1 pptv according to our model calculations minutes after exhaust, the gas phase production of HNO_3 via $NO_2 + OH + M \rightarrow HNO_3 + M$ is several orders of magnitude smaller than that of (R1) and is omitted in equation (1). Contributions of N_2O_5 and $BrONO_2$ hydrolysis to HNO_3^c are much smaller than those from (R1) in the plume and are neglected. These facts show that the (R1) reaction is a principal source of HNO_3 in the Athena-2 plume.

[9] We assume that the amount of HNO_3 condensed per unit of area should be the same for any particle size. This assumption determines partitioning of HNO_3^c among alumina particles. Equation (1) contains two unknown parameters, namely, τ_1 and α_1. While we can not determine them simultaneously, we can bracket the values of τ_1 for the smallest (=0) and largest (=1) values of α_1. Figures 2d–2e show the evolution of HNO_3 in gas and condensed phases in the plume for $\alpha_1 = 1$.

[10] Comparing model calculations and measurements, one should keep in mind that: (1) the JPL laser hygrometer measures only gas-phase H_2O and (2) the NOAA CIMS measures both the gas-phase and condensed HNO_3. The HNO_3 instrument samples through a forward-facing sub-isokinetic inlet, which causes particles with diameter larger than 0.1 μm to be significantly enhanced in the sample flow. Thus, any condensed HNO_3 in the plume is enhanced by the factor EF(r) for particles with radius r. Thus, knowing the amount of HNO_3^g and HNO_3^c in our model, the apparent amount of HNO_3^{app} as seen by the CIMS is determined by

$$HNO_3^{app} = HNO_3^g + HNO_3^c \frac{\sum_{i=1}^{40} n_i r_i^2 EF_i}{\sum_{i=1}^{40} n_i r_i^2}. \quad (2)$$

Here EF_i and n_i are the CIMS enhancement factor and the number of particles in the ith bin (shown in Figure 2c), respectively. Figure 2f compares apparent values of nitric acid according to the measurements (black symbols) and model calculations (color lines). A good agreement between modeled and measured HNO_3^{app} values is not surprising, since we adjusted τ_1 for obtaining agreement. The derived values of τ_1 are shown in Table 1, ranging from 17 to 52 min and from 5 to 12 min for the cases without and with direct uptake of HNO_3 vapor by alumina particles, respectively. The derived values of τ_1 for plume 1 are an outlier and discarded in our conclusions.

2.4. H_2O

[11] Since there is no photochemical production of H_2O^c in the plume, the evolution of H_2O^c is described by

$$\frac{dH_2O^c}{dt} = \frac{SAD\alpha_2 v_2 H_2O^g}{4} - \frac{H_2O^c}{\tau_2}. \quad (3)$$

Again, we have two unknowns (α_2 and τ_2) and one equation (3). We performed several sensitivity studies by

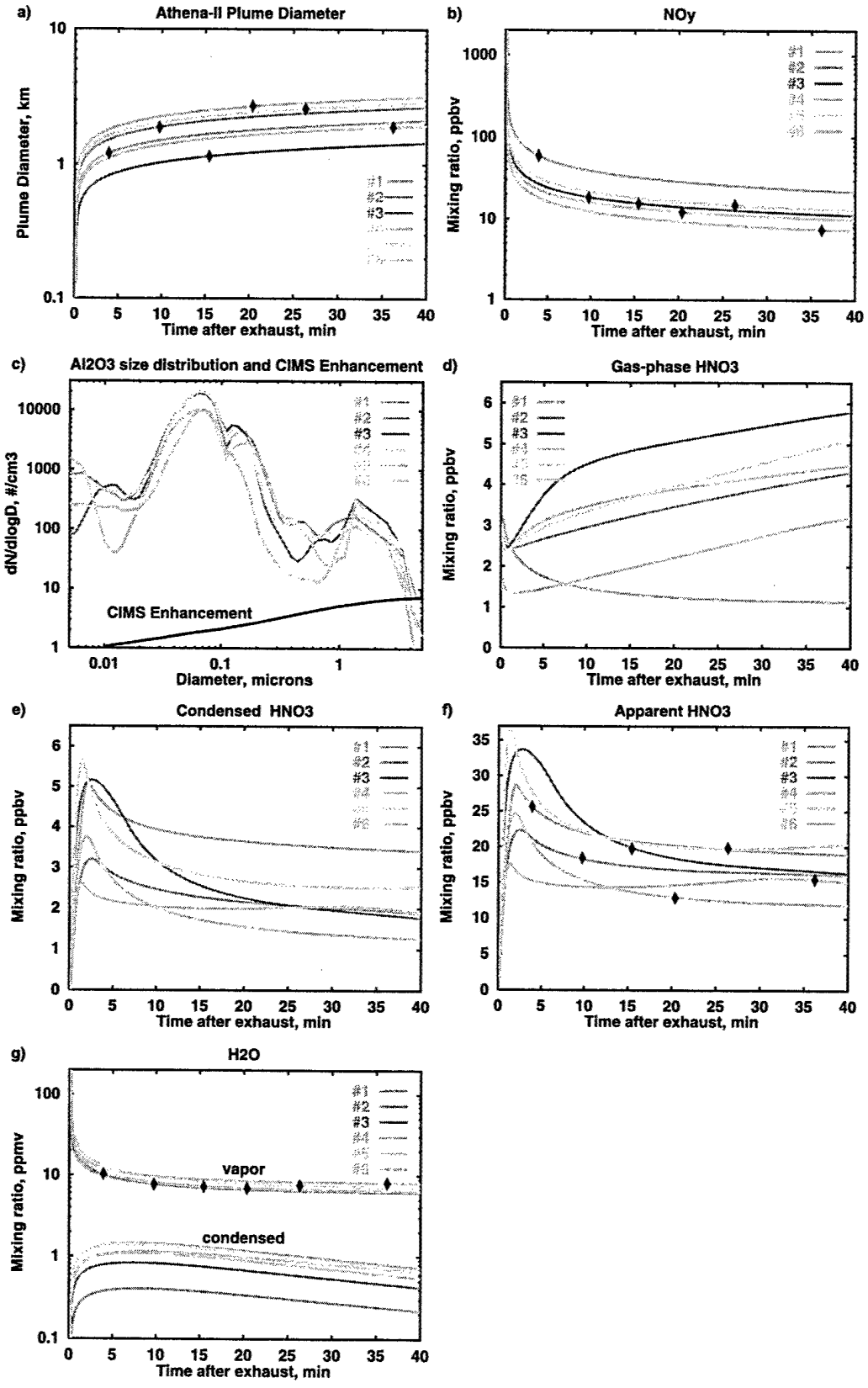
a)
Athena-II Plume Diameter
Plume Diameter, km
Time after exhaust, min
b)
NOy
Mixing ratio, ppbv
Time after exhaust, min
#1
#2
#3
c)
Al2O3 size distribution and CIMS Enhancement
dN/dlogD, #/cm3
CIMS Enhancement
Diameter, microns
d)
Gas-phase HNO3
Mixing ratio, ppbv
Time after exhaust, min
e)
Condensed HNO3
Mixing ratio, ppbv
Time after exhaust, min
f)
Apparent HNO3
Mixing ratio, ppbv
Time after exhaust, min
g)
H2O
Mixing ratio, ppmv
vapor
condensed
Time after exhaust, min

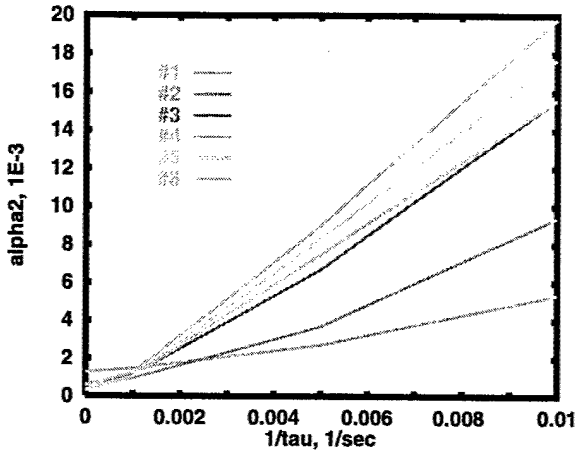

Figure 3. The α_2-$1/\tau$ relations for H_2O in Athena-2 plumes.

deriving α_2 for the τ_2 values of 100, 200, 1000 s, and ∞. The results are presented in Figure 3. The minimum values of α_2 for infinite τ_2 (i.e. without H_2O desorption from alumina particles) are shown in Table 1 and are in the range of $(2.7-12.5) \times 10^{-4}$. Extrapolating our results up to $\alpha_2 = 1$ using the derived slope of $d\alpha_2/d(1/\tau) = 2$ s, one gets τ_2 of 0.5 s. These τ_2 values are of relevance for H_2O uptake by liquid water in the stratosphere [*Li et al.*, 2001]. Table 1 shows that our calculations predict about 0.5 to 1.0 ppmv of condensed H_2O in the plume. This is in close agreement with the observations by *Gates et al.* [2002] and *Herman et al.* [2001].

2.5. Sensitivity Studies

[12] We investigate the sensitivity of the results given in Table 1 to the uncertainties of (1) particle measurements, (2) initial partitioning of chlorine species between Cl_2 and HCl, and (3) initial condensed H_2O on alumina particles. Table 2 summarizes our findings assuming $\alpha_1 = 1$ and $\tau_2 = 1000$ s for all calculations here.

[13] Alumina particle measurements in the plume by NMASS, FCASS, and MASP may have a total uncertainty of 100%, which affects the Al_2O_3 SAD and consequently the derived values of α and τ for H_2O and HNO_3. We made sensitivity calculations with increased and decreased alumina SAD by a factor of 2 and show our results for doubled alumina SAD in Table 2 (4th and 5th columns). The change in alumina SAD leads to a change of the (R1) reaction rate (which is a main source of HNO_3^c in the plume) and affects the partitioning of H_2O and HNO_3 between condensed and gas phases. For larger Al_2O_3 SAD, larger values of H_2O^c and HNO_3^c and smaller values of τ_1 and τ_2 are required in order to explain the measurements. In the case of H_2O, an increase (decrease) of SAD by a factor of two decreases (increases) the values of τ_2 by the same factor (compare 3rd and 5th columns of Table 2). In the case of HNO_3, its

Table 2. Sensitivity of τ_1 and α_2 to Doubling Al_2O_3 SAD, Doubling Initial Cl_2, and Initial 0.5 ppmv of Condensed H_2O, Assuming $\alpha_1 = 1$ and $\tau_2 = 1000$ s[a]

	Baseline		2SAD			
Plume	τ_1	α_2	τ_1	α_2	$2Cl_2$[b] τ_1	0.5 ppmv[c] α_2
1	103	14.7	11.3	7.3	13.7	1.3
2	15.0	9.4	8.5	4.7	4.5	2.9
3	6.3	11.2	3.8	5.6	3.4	8.2
4	5.4	12.6	3.0	6.3	2.0	10.5
5	7.2	10.4	4.1	5.2	2.3	9.3
6	9.1	10.6	4.5	5.3	6.8	9.7

[a]Sensitivity of τ_1 is given in minutes, and sensitivity of α_2 values are $\times 10^{-4}$.
[b]α_2 is the same as in the baseline case.
[c]τ_1 is the same as in the baseline case.

photochemical production is involved which complicates the dependence of τ_1 on SAD. However, τ_1 is also reduced by almost a factor of 2 for doubled alumina SAD (compare 2nd and 4th columns of Table 2). Similar conclusions are obtained from the model runs with alumina SAD reduced by a factor of 2 (not shown in Table 2).

[14] Near-field rocket combustion models [*Zittel*, 1994] predict that 35% by mass of emitted chlorine should be present as Cl_2 at 18 km in the Athena-2 plume. Since our plume calculations, constrained by the WB-57F measurements, show that only 5–15% of chlorine is converted to Cl_2 in order to be consistent with the ozone measurements, we investigate how doubling of our initial Cl_2 affects the values of τ_1 (the values of α_2 remain unchanged). Initial Cl_2 and τ_1 are linked, since higher values of Cl_2 lead to larger values of ClO and $ClONO_2$, thus accelerating the formation of HNO_3 and shortening τ_1. The 6th column of Table 2 shows that the link between initial partitioning of the emitted chlorine species and required residence time of HNO_3 on alumina particles is quite pronounced. However, one should keep in mind that this sensitivity test was a bit hypothetical, since the ozone values obtained in these calculations were considerably smaller than those measured by the WB-57F. Nevertheless, it is of interest to perform this sensitivity test since the discrepancy between our derived Cl_2 fraction and the fraction predicted by the rocket combustion models is larger than the expected uncertainties in the rocket combustion models. The source of this discrepancy is unclear but our results suggest that the combustion models may significantly overpredict the production of Cl_2. In order to validate near-field and our far-field calculations of chlorine partitioning in the SRM exhaust, one should have simultaneous measurements of ClO and HCl. In situ HCl measurements may be also valuable for the study of HCl interactions with alumina particles in rocket plumes and with other aerosol in the background atmosphere.

[15] Near-field calculations also show a possibility for H_2O condensation onto alumina particles during the first few seconds after exhaust. In order to address this possi-

Figure 2. (opposite) Temporal evolution of plume diameter (Figure 2a), NO_y (Figure 2b), HNO_3 (Figures 2d–2f, $\alpha_1 = 1$), and H_2O (Figure 2g, $\tau_2 = 1000$ s) in the Athena-2 plumes. Measured size distribution of alumina particles and CIMS enhancement factor are shown in Figure 2c. Plume events are color-coded as shown and measurements are shown by the black symbols.

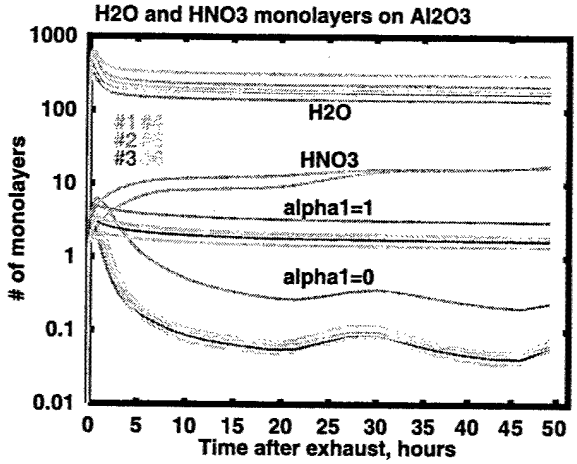

Figure 4. Number of H_2O and HNO_3 monolayers on Athena-2 alumina particles during first two days after exhaust. Plume events are color coded as shown.

bility in our model calculations, which overlook plume processes during the first 5 s downstream, we performed additional model runs with the initial condensed phase H_2O equals to 0.5 ppmv. Comparison of the 3rd and 7th columns of Table 2 shows the effect of initial H_2O^c on α_2, which is larger for younger plumes and smaller for older plumes, hence showing that the initial conditions become less important with time. For example, for plume 6 the effect of initial condensed H_2O leads to reduction of α_2 by only 10%. Since condensed water does not affect the reaction probability of (R1) in our calculations, the values of τ_1 remain unchanged in this sensitivity test.

2.6. Implications

[16] What will happen with coverage of alumina particles under background conditions? To answer this question, we present 2-day-long model runs. Assuming $\sigma_2 = 10^{-15}$ and $\sigma_1 = 2 \times 10^{-15}$ cm^2 for the areas of one molecule of H_2O and HNO_3 [*Grassian*, 2002], respectively, and knowing the evolution of Al_2O_3 SAD with time from our model calculations, we obtain the number of H_2O (n_2^m) and HNO_3 (n_1^m) monolayers on alumina particles shown in Figure 4. Our results indicate that hundreds of H_2O and up to several HNO_3 monolayers may cover alumina particles in the Athena-2 plumes days after emission. These asymptotic values show the coverage of alumina particles under background conditions and may be confirmed by the following calculations. Assuming that $dH_2O^c/dt = 0$ under background conditions and using equation (3), one gets

$$n_2^m = \frac{\sigma_2 H_2O^c}{SAD} = \frac{\sigma_2 \tau_2 \alpha_2 v_2 H_2O^g}{4}, \quad (4)$$

which gives $n_2^m = 148$ monolayers for $\tau_2 = 10^3$ s, $\alpha_2 = 10^{-3}$, $v_2 = 49400$ cm/s, and $H_2O = 5$ ppmv $= 1.2 \times 10^{13}$ #/cm^3 at 70 hPa. Using the same approach for HNO_3, one gets

$$n_1^m = \frac{\sigma_1 \tau_1 \left(\gamma v ClONO_2^g + \alpha_1 v_1 HNO_3^g\right)}{4}. \quad (5)$$

The values of n_1^m range from 0.3 ($\alpha_1 = 0$) to 13 ($\alpha_1 = 1$) monolayers of HNO_3 for typical values of $ClONO_2$ (=0.5 ppbv) and HNO_3 (=1.4 ppbv) and assuming τ_1 of 1000 s and 300 s for $\alpha_1 = 0$ and $\alpha_2 = 1$, respectively. These values of n_1^m are consistent with those shown in Figure 4. Assuming that surface properties of alumina particles are the same for all solid-fueled rockets, our results for n_1^m and n_2^m are valid for the Space Shuttle too, which is the main source of alumina in the global stratosphere.

[17] One also can obtain from equations (1) and (3) the amount of condensed H_2O^c and HNO_3^c, which is of the order of 10^5–10^6 #/cm^3 and 10^2–10^3 #/cm^3, respectively, assuming the Al_2O_3 SAD of 4×10^{-4} μm^2/cm^3 [*Danilin et al.*, 2001b, Figure 5] at 18 km at 40°N.

2.7. Discussion

[18] The hydrophilic properties of the Athena-2 exhaust show that there are three stages in the evolution of alumina particles. First, the fresh alumina particles become covered very quickly primarily by H_2O during the first minute after emission. Initial uptake coefficients of H_2O and HNO_3 are of the order of 10^{-4}–10^{-3} [*Grassian*, 2002] and the reaction probability for (R1) is equal to 0.02 [*Molina et al.*, 1997]. Second, alumina particles are covered by several hundred monolayers of H_2O containing small amounts of HNO_3 and, likely, other soluble acids (H_2SO_4, HCl) [*Van Doren et al.*, 1990; *Robinson et al.*, 1998]. Within minutes after exhaust the alumina particles should behave like mildly acidic water droplets with α_2 and γ of an order of 0.1–1 [*Li et al.*, 2001; *Shi et al.*, 2001]. Third, hours after emission, when H_2O in the plume relaxes to its ambient values, the fate of liquid coverage strongly depends on ambient conditions. For example, if the vapor pressure of H_2O on alumina particles exceeds the ambient H_2O partial pressure, H_2O may evaporate changing γ from 0.1–1 to 0.02.

[19] Perhaps, the most surprising results of the Athena-2 plume measurements is a persistence of condensed H_2O and HNO_3 on alumina particles under temperature conditions that are considerably higher than the NAT or ice thresholds. While the evaporation of H_2O from alumina particles may be decreased by the presence of HNO_3^c [e.g., *Warshawsky et al.*, 1999], it is not clear whether this is enough to explain the measurements. The calculations here represent constant values of temperature and pressure (208.1 K at 70 hPa and 200.2 K at 97 hPa) and are valid in the lower stratosphere only. Since a dependence of γ, α_1, α_2, τ_1, and τ_2 on number of H_2O and HNO_3 monolayers on alumina particles is unknown, our calculations assume constant values of these parameters. Further laboratory measurements are required to infer these dependences, incorporate them in a model, and check our results.

[20] An additional caveat is that the properties of the emitted alumina particles may differ from those used in laboratory studies. For example, current laboratory data are available for hexagonal α-Al_2O_3 [e.g., *Molina et al.*, 1997] and it is not obvious that they are valid for cubic γ-Al_2O_3, which may be formed in solid-fueled rocket exhaust and is a more reactive form of alumina [*Dai et al.*, 1997].

[21] Our analysis also shows that small particles (i.e., d < 0.7 μm) account for almost 2% of emitted alumina mass based on the size distribution measured by the NMASS, FCAS, and MASP instruments. It is very important to know

the fraction of alumina mass in submicron range [*Danilin et al.*, 2001b], since these small particles have a long residence time in the stratosphere and are available longer for background chlorine activation via (R1) on their surface, thus affecting ozone. Assuming that Space Shuttle and Titan-IV rockets have the same size distribution of alumina particles as Athena-2 and applying results from the global model [*Danilin et al.*, 2001b, Table 2], the ozone depletion potential (ODP) of alumina emitted by these rockets could be as large as 0.1 for $\gamma = 0.02$. Our study shows that alumina particles may be covered by water and nitric acid, raising the possibility that the (R1) reaction probability γ is larger than 0.02 under background conditions. If so, the estimated ODP of alumina particles may exceed the value of 0.2. Further laboratory and field measurements are required in order to better quantify alumina particle effects on the ozone layer.

3. Summary

[22] Athena-2 rocket plume measurements during the ACCENT campaign show that H_2O and HNO_3 are condensed onto alumina particles. Quantifying their uptake using the AER plume model constrained by all relevant measurements, we found that (1) the H_2O uptake coefficient is larger than 3×10^{-4}, (2) HNO_3 molecules reside for 5–52 min on Al_2O_3 surfaces, and (3) alumina particles in the background atmosphere may be covered by 100–200 monolayers of H_2O and 0.1–10 monolayers of HNO_3. These values are uncertain by at least a factor of two and require additional laboratory studies. Once the interactions of alumina particles with H_2O, HNO_3, and other acids are understood based on laboratory studies and field measurements, new model calculations should be made in order to estimate effects of alumina particles on the atmosphere.

[23] **Acknowledgments.** We thank the WB-57F crew for making these measurements. Efforts of C. A. Brock, J. W. Elkins, and F. L. Moore are appreciated. This work was supported in part by the NASA AEAP and USAF. Work at JPL, Caltech, was done under contract to NASA. We thank two anonymous reviewers for their comments.

References

Baumgardner, D. G., J. E. Dye, B. Gandrud, K. Barr, K. Kelly, and K. R. Chan, Refractive indices of aerosols in the upper troposphere and lower stratosphere, *Geophys. Res. Lett.*, *23*, 749–752, 1996.

Dai, Q., G. N. Robinson, and A. Freedman, Reactions of halomethanes with γ-alumina surfaces, 1, An infrared spectroscopic study, *J. Phys. Chem. B*, *101*, 4940–4946, 1997.

Danilin, M. Y., M. K. W. Ko, and D. K. Weisenstein, Global implications of ozone loss in a space shuttle wake, *J. Geophys. Res.*, *106*, 3591–3601, 2001a.

Danilin, M. Y., R.-L. Shia, M. K. W. Ko, D. K. Weisenstein, N. D. Sze, J. J. Lamb, T. W. Smith, P. D. Lohn, and M. J. Prather, Global stratospheric effects of the alumina emissions by solid-fueled rocket motors, *J. Geophys. Res.*, *106*, 12,727–12,738, 2001b.

Fahey, D. W., et al., In situ observations in aircraft exhaust plumes in the lower stratosphere at midlatitudes, *J. Geophys. Res.*, *100*, 3065–3074, 1995.

Gates, A. M., D. W. Toohey, A. Rutter, P. D. Whitefield, D. E. Hagan, M. N. Ross, T. L. Thompson, R. L. Herman, R. R. Friedl, and L. M. Avallone, In situ measurements of carbon dioxide, 0.37–4.0 μm particles, and water vapor in the stratospheric plumes of three rockets, *J. Geophys. Res.*, *107*(D22), 4649, doi:10.1029/2002JD002121, 2002.

Grassian, V. H., Chemical reactions of nitrogen oxides on the surface of oxide, carbonate, soot, and mineral dust particles: Implications for chemical balance of the troposphere, *J. Phys. Chem. A*, *106*, 860–877, 2002.

Herman, R. L., R. R. Friedl, and B. W. Gandrud, Water vapor enhancements in an Athena II rocket plume, *Eos Trans. AGU*, *82*(47), Fall Meet. Suppl., F135, 2001.

Jackman, C. H., D. B. Considine, and E. L. Fleming, A global modeling study of solid rocket aluminum oxide emission effects on stratospheric ozone, *Geophys. Res. Lett.*, *25*, 907–910, 1998.

Ko, M. K. W., N. D. Sze, and M. J. Prather, Better protection of the ozone layer, *Nature*, *367*, 505–508, 1994.

Li, Y. Q., P. Davidovits, Q. Shi, J. T. Jayne, C. E. Kolb, and D. R. Worsnop, Mass and thermal accommodation coefficients of H_2O(g) on liquid water as a function of temperature, *J. Phys. Chem. A*, *105*, 10,627–10,634, 2001.

May, R. D., Open-path, near-infrared tunable diode laser spectrometer for atmospheric measurements of H_2O, *J. Geophys. Res.*, *103*, 19,161–19,172, 1998.

Molina, M. J., L. T. Molina, R. Zhang, R. F. Meads, and D. D. Spencer, The reaction of $ClONO_2$ with HCl on aluminum oxide, *Geophys. Res. Lett.*, *24*, 1619–1622, 1997.

Popp, P. J., et al., The emission and chemistry of reactive nitrogen species in the plume of an Athena II solid-fuel rocket motor, *Geophys. Res. Lett.*, *29*(18), 1887, doi:2002GL015197, 2002.

Prather, M. J., M. M. Garcia, A. R. Douglas, C. H. Jackman, M. K. W. Ko, and N. Dak Sze, The space shuttle's impact on the stratosphere, *J. Geophys. Res.*, *95*, 18,583–18,590, 1990.

Richard, E. C., et al., Severe chemical ozone loss inside the Arctic polar vortex during winter 1999–2000 inferred from in situ airborne measurements, *Geophys. Res. Lett.*, *28*, 2197–2200, 2001.

Robinson, G. N., D. R. Worsnop, J. T. Jayne, C. E. Kolb, E. Swartz, and P. Davidovits, Heterogeneous uptake of HCl by sulfuric acid solutions, *J. Geophys. Res.*, *103*, 25,371–25,381, 1998.

Ross, M. N., et al., Observation of stratospheric ozone depletion associated with Delta-II rocket emissions, *Geophys. Res. Lett.*, *27*, 2209–2212, 2000.

Sander, S. P., et al., Chemical kinetics and photochemical data for use in stratospheric modeling: Evaluation 13, *JPL Publ.*, *00-3*, 2000.

Schmid, O., J. M. Reeves, J. C. Wilson, C. Wiedinmyer, C. Brock, D. W. Toohey, L. M. Avallone, A. Gates, and M. N. Ross, Size-resolved measurements of particle emission indices in the stratospheric plume of a solid-fueled rocket motor, *J. Geophys. Res.*, 107, doi:10.1029/2002JD002486, in press, 2002.

Shi, Q., J. T. Jayne, C. E. Kolb, and D. R. Worsnop, Kinetic model for reactions of $ClONO_2$ with H_2O and HCl and HOCl with HCl in sulfuric acid solutions, *J. Geophys. Res.*, *106*, 24,259–24,274, 2001.

Van Doren, J. M., L. R. Watson, P. Davidovits, D. R. Worsnop, M. S. Zahniser, and C. E. Kolb, Temperature dependence of the uptake of HNO_3, HCl, and N_2O_5 by water droplets, *J. Phys. Chem.*, *94*, 3265–3269, 1990.

Warshawsky, M. S., M. A. Zondlo, and M. A. Tolbert, Impact of nitric acid on ice evaporation rates, *Geophys. Res. Lett.*, *26*, 823–826, 1999.

World Meteorological Organization (WMO), Scientific assessment of ozone depletion: 1991, *Rep. 25*, chap. 10, Geneva, 1992.

Zittel, P. F., Computer model predictions of the local effects of large solid-fueled rocket motors on stratospheric ozone, *Tech. Rep. TR-94 (4321)-9*, Aerospace Corp., El Segundo, Calif., 1994.

L. M. Avallone and D. W. Toohey, Program in Atmospheric and Oceanic Sciences, University of Colorado, Boulder, CO 80309, USA.

D. G. Baumgardner, Center of Atmospheric Sciences, National University of Mexico, 04510 Mexico City DF, Mexico.

M. Y. Danilin, The Boeing Company, MC 0R-RC, P. O. Box 3707, Seattle, WA 98124-2207, USA. (danilin@h2o.ca.boeing.com)

D. W. Fahey, P. J. Popp, and T. L. Thompson, Aeronomy Laboratory, NOAA, 325 Broadway, Boulder, CO 80303, USA.

R. R. Friedl and R. L. Herman, Jet Propulsion Laboratory, NASA, 4800 Oak Grove Drive, Pasadena, CA 91109, USA.

M. K. W. Ko, NASA Langley Research Center, MS 401B Hampton, VA 23681-2199, USA.

C. E. Kolb, Aerodyne Research, Inc., 45 Manning Road, Billerica, MA 01821, USA.

J. M. Reeves, O. Schmid, and J. C. Wilson, Department of Engineering, University of Denver, 2390 S. York Street, Denver, CO 80208, USA.

B. A. Ridley, National Center for Atmospheric Research, P. O. Box 3000, Boulder, CO 80303, USA.

M. N. Ross, The Aerospace Corporation Los Angeles, P. O. Box 92957, Los Angeles, CA 90009, USA.

O. Schmid, Max Planck Institute for Chemistry, P. O. Box 3060, D-55020 Mainz, Germany.

GEOPHYSICAL RESEARCH LETTERS, VOL. 27, NO. 15, PAGES 2209-2212, AUGUST 1, 2000

Observation of Stratospheric Ozone Depletion Associated With Delta II Rocket Emissions

M. N. Ross[1], D. W. Toohey[2], W. T. Rawlins[3], E. C. Richard[4], K. K. Kelly[4], A. F. Tuck[4], M. H Proffitt[5], D. E. Hagen[6], A. R. Hopkins[6], P. D. Whitefield[6], J. R. Benbrook[7], and W. R. Sheldon[7]

Abstract. Ozone, chlorine monoxide, methane, and submicron particulate concentrations were measured in the stratospheric plume wake of a Delta II rocket powered by a combination of solid (NH_4ClO_4/Al) and liquid (LOX/kerosene) propulsion systems. We apply a simple kinetics model describing the main features of gas-phase chlorine reactions in solid propellant exhaust plumes to derive the abundance of total reactive chlorine in the plume and estimate the associated cumulative ozone loss. Measured ozone loss during two plume encounters (12 and 39 minutes after launch) exceeded the estimate by about a factor of about two. Insofar as only the most significant gas-phase chlorine reactions are included in the calculation, these results suggest that additional plume wake chemical processes or emissions other than reactive chlorine from the Delta II propulsion system affect ozone levels in the plume.

1. Introduction

Rockets used by the space launch industry employ a number of different propellant combinations and emit a variety of exhaust products directly into the stratosphere. While rocket exhaust currently represents a small fraction of the total impact of industrial activity on the stratosphere, prudence requires that we carefully evaluate its impact. Space launch traffic in general is widely expected to increase during coming decades so that the stratospheric impact of rocket emissions from all propellant types will increase. Previous investigations have focused mainly on the stratospheric impact of large solid rocket motors (SRMs) using ammonium perchlorate (NH_4ClO_4) oxidizer. Recent stratospheric measurements have shown that large solid fueled rockets dramatically perturb stratospheric ozone in regions covering up to several hundred square kilometers for several hours after launch [Ross et al., 1997b].

Solid fueled rockets, however, represent only a portion of the emission inventory of the space launch industry. Another widely used propellant combination is liquid oxygen and kerosene (LOX/RP; RP refers to RP-1 or RG-1, kerosene distillations widely used as rocket fuel.) Careful study of LOX/RP combustion emissions is justified for several reasons. LOX/RP exhaust accounts for a significant fraction (about one fourth by mass in 1998) of the total stratospheric emission by rockets and several powerful LOX/RP rockets in development will increase the relative impact of these emissions. In this paper we present measurements obtained in the stratospheric plume wakes of a Delta II rocket that provide evidence that reactive chlorine gas may not be the only chemically active component of the Delta II emission.

2. Plume Wake Measurements and Analysis

The Delta II plumes were sampled following daytime launches on November 7, 1996 (1600 UT) from Cape Canaveral Air Station (28° 33' N, 80° 18' W) and on May 17, 1998 (2316 UT) from Vandenberg Air Force Base (120° 37' W, 34° 48' N). The altitudes of the plume encounters varied between 18 and 18.6 km. Measurements included O_3 [Sen et al., 1996] (University of Houston) and total (volatile and nonvolatile) aerosol concentrations [Ross et al., 1999] in 1996 and ClO [Pierson et al., 1999], CH_4, three independent O_3 measurements [Sen et al., 1996] (University of Houston); [Proffitt et al., 1989] (NOAA); and [Proffitt and Rawlins, 1998] (PSI) and total aerosol concentrations [Ross et al., 1999] in 1998. Following each launch, the WB-57F aircraft intercepted the plume wake six times. Only the 1998 data is comprehensive enough to support significant conclusions regarding the details of plume wake chemistry and we focus on that data shown in Figure 1. The plume encounters are clearly visible as large departures from the background for all species except CH_4, which shows a modest decrease only during the fifth encounter. The sixth encounter does not conform with the trends in composition (progressively greater ozone loss) and duration (progressively longer) observed in the preceding encounters, apparently because the aircraft intercepted an edge of the main plume. Since the encounters occurred at slightly different altitudes (between 18 and 18.6 km), the aircraft sampled distinct plume segments.

Representative of the first three encounters, Figure 2 shows expansions of the second encounter when the plume was 12 minutes old. At the center of the generally symmetric plume, ozone concentration was reduced by 70% from the

[1]M. N. Ross, Environmental Systems Directorate, The Aerospace Corporation, PO Box 92957, Los Angeles CA 90009.
[2]D. W. Toohey, Program in Atmospheric Sciences, University of Colorado, Boulder CO 80309
[3]W. T. Rawlins, Physical Sciences, Incorporated, 20 New England Business Center, Andover MA 01810
[4]E. C. Richard, K. K. Kelly, A. F. Tuck, Aeronomy Laboratory, NOAA, 325 Broadway, Boulder CO 80303
[5]M. H. Proffitt, The Environmental Division, World Meteorological Organization, 7 bis, Aveneue de la Paix, Geneva, Switzerland
[6]P. D. Whitefield, D. E. Hagen, A. R. Hopkins, Cloud and Aerosol Sciences Laboratory, University of Missouri-Rolla, Rolla MO 65401
[7]J. R. Benbrook and W. R. Sheldon, Physics Department, University of Houston, Houston TX 77204

Paper number 1999GL011159.
0094-8276/00/1999GL011159$05.00

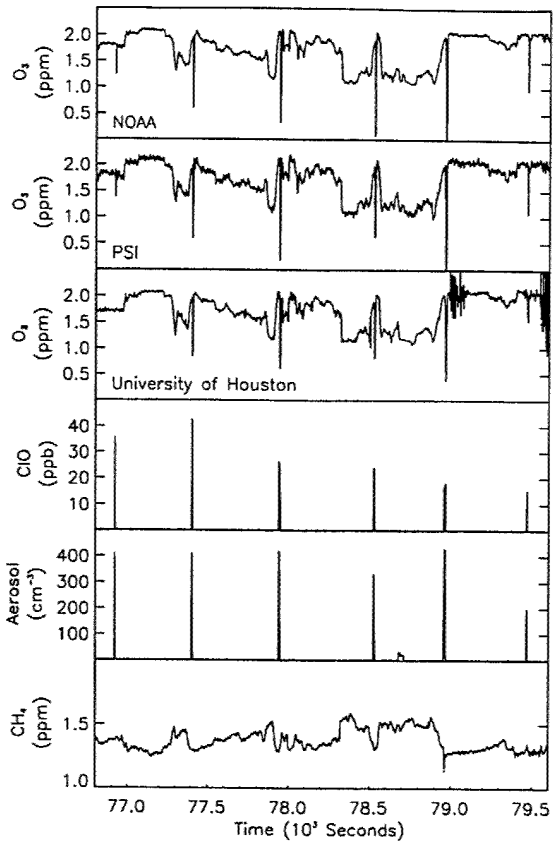

Figure 1. Time series of measurements during the 46 minute period that included the six plume encounters. Units are mixing ratio in parts per million by volume (ppmv), parts per billion by volume (ppbv), and total (volatile and nonvolatile) aerosol number density in the size range 0.3 to 4 μm. The small aerosol event after the fourth plume encounter is interpreted as an encounter with the WB-57F's own exhaust. The bottom axis is Universal Time on 17 May 1998.

background value. The maximum ClO concentration was 45 ± 15 ppbv, about a factor 20 greater than in the South Polar springtime vortex [Pierson et al., 1999]. Methane concentration in the plume was not different from the ambient background. A proposed description of gas phase SRM plume photochemistry features a ClO dimer catalytic cycle unique to warm (≈ 215 K) SRM plumes [Ross, 1996; Ross et al., 1997b]:

$$\begin{aligned} &2x\,(Cl + O_3 \rightarrow ClO + O_2)\\ &ClO + ClO + M \rightarrow Cl_2O_2 + M\\ &Cl_2O_2 + Cl \rightarrow Cl_2 + ClOO\\ &Cl_2 + \hbar\nu \rightarrow 2Cl\\ &ClOO + M \rightarrow Cl + O_2 + M\\ &\text{Net: } 2O_3 \rightarrow 3O_2. \end{aligned} \qquad (1)$$

The set of reactions (1) can reasonably be taken to describe the main aspects of SRM plume kinetics because all of the chlorine species are in significant excess (≈ 10^2) of ambient species that might play a role in the plume kinetics (HO_X and NO_X for example) and because all other Cl_X family reactions are slow compared to those that make up (1). Our desire is not to explain all the details of the plume kinetics (nor is that presently possible, given the many uncertainties regarding the actual Delta II emissions). Rather, we seek to evaluate the ability of the reaction set (1) to explain the observed ozone loss.

Within a few minutes after launch, the principal chlorine species are in a slowly varying steady-state and the reactions (1) can be solved to yield a relationship between [ClO] (in units of cm^{-3}) and total reactive chlorine $[Cl_X] \equiv [ClO] + [Cl] + 2[Cl_2] + 2[Cl_2O_2]$:

$$[Cl_X] = 1.5\,[ClO] + 5.4 \times 10^{-11}\,[ClO]^2 \qquad (2)$$

The numerical coefficients were determined using DeMore et al. [1997] for temperature and pressure equal to 215 K and 65 mbar, respectively, and ambient O_3 mixing ratio of 2 ppmv; the coefficients are not greatly sensitive to these conditions. Detailed kinetics calculations [Rawlins et al., 1998] verify the analytic result (2) and show that about 90% of the Cl_X is in the form of Cl_2 during the steady-state. We average the plume ingress and egress data (to reduce the influence of small scale structure in the plume) and fit a linear expression to describe the radial dependence of [ClO] and, therefore, $[Cl_X]$ using (2). Integrating derived $[Cl_X]$ across the plume and taking into account the known uncertainty in measured [ClO] we find that the total abundance of reactive chlorine in the plume, $\{Cl_X\}$ (brackets indicating the horizontal integration), does not exceed 0.9 moles per meter of altitude (Mm^{-1}).

When Cl_X is greatly in excess of O_3, Cl_2 photolysis (J = 0.22 min^{-1} for the relevant local conditions, P. F. Zittel and P. K. Swaminathan, personal communications) controls the rate of ozone destruction and the horizontally integrated cumulative ozone loss in the plume and $\{\Delta O_3\}$ during a time Δt can be approximated by

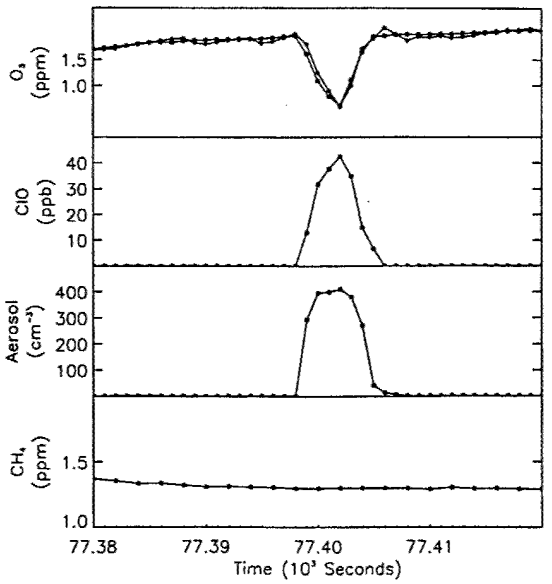

Figure 2. Expanded time series for the second plume encounter. In the topmost panel data from the NOAA and PSI instruments are given by circles and squares, respectively. Data rates are 1 Hz except for CH_4 which is 0.5 Hz. The bottom axis is Universal Time on 17 May 1998. WB-57F airspeed is about 190 ms^{-1}.

GEOPHYSICAL RESEARCH LETTERS, VOL. 29, NO. 18, 1887, doi:10.1029/2002GL015197, 2002

The emission and chemistry of reactive nitrogen species in the plume of an Athena II solid-fuel rocket motor

P. J. Popp,[1,2] B. A. Ridley,[3] J. A. Neuman,[1,2] L. M. Avallone,[4] D. W. Toohey,[5]
P. F. Zittel,[6] O. Schmid,[7] R. L. Herman,[8] R. S. Gao,[1] M. J. Northway,[1,2] J. C. Holecek,[1,2]
D. W. Fahey,[1,2] T. L. Thompson,[1] K. K. Kelly,[1] J. G. Walega,[3] F. E. Grahek,[3]
J. C. Wilson,[7] M. N. Ross,[6] and M. Y. Danilin[9]

Received 22 March 2002; revised 20 August 2002; accepted 2 May 2002; published 26 September 2002.

[1] In situ measurements of NO, NO_y, HNO_3, ClO, CO_2, H_2O and particles were made in the plume of an Athena II solid-fuel rocket motor (SRM) with instruments onboard the NASA WB-57F high-altitude aircraft. By normalization to CO_2, the NO_y emission index was calculated to be 2.7±0.6 g NO_2 (kg fuel)$^{-1}$. HNO_3 is a significant and evolving component plume NO_y. The principal source of HNO_3 is thought to be the heterogeneous reaction between $ClONO_2$ and HCl on emitted alumina particles. These measurements provide the first experimental evidence for the production of HNO_3 and the activation of chlorine on SRM-emitted alumina particles in the lower stratosphere. *INDEX TERMS:* 0305 Atmospheric Composition and Structure: Aerosols and particles (0345, 4801); 0322 Constituent sources and sinks; 0340 Middle atmosphere—composition and chemistry. **Citation:** Popp, P. J., et al., The emission and chemistry of reactive nitrogen species in the plume of an Athena II solid-fuel rocket motor, *Geophys. Res. Lett.*, *29*(18), 1887, doi:10.1029/2002GL015197, 2002.

1. Introduction

[2] Current SRMs release energy through the oxidation of aluminum in the presence of ammonium perchlorate (NH_4ClO_4), resulting in the emission of combustion products directly into the stratosphere during launch [*Prather et al.*, 1990]. Nitric oxide (NO) is produced directly by the SRM combustion process and in secondary combustion processes known as afterburning when ambient air is entrained into the hot exhaust plume [*Bennet and McDonald*, 1994]. NO production and reaction in SRM plumes is not well studied. Although an SRM NO emission index of 7 g of NO (as equivalent NO_2) per kg of fuel has been reported, this value did not account for the post-emission oxidation of NO in the plume [*Potter*, 1977].

[3] Observations of chlorine monoxide (ClO) in a stratospheric SRM plume [*Ross et al.*, 2000] suggest that emitted NO is oxidized and subsequently forms chlorine nitrate ($ClONO_2$). Laboratory studies have shown that $ClONO_2$ could then react with hydrogen chloride (HCl) on alumina (Al_2O_3) particles via

$$ClONO_2 + HCl \xrightarrow{Al_2O_3} Cl_2 + HNO_3 \qquad (R1)$$

[*Molina et al.*, 1997] to effectively convert NO to nitric acid (HNO_3). It should also be noted that (R1) provides a means of converting HCl, the primary chlorine species emitted by SRMs [*Prather et al.*, 1990], to active chlorine. The severe ozone (O_3) loss observed locally in SRM plumes is known to result from reactions involving active chlorine species [*Ross et al.*, 1997a, 1997b]. While it has been suggested that heterogeneous chlorine activation could play a role in plume O_3 loss [*Ross et al.*, 2000], the contribution of (R1) to active chlorine in the plume requires further observational support.

[4] We report here in situ measurements of total reactive nitrogen (NO_y = NO + NO_2 + $ClONO_2$ + $2N_2O_5$ + HNO_3 ...), NO, and HNO_3 in the stratospheric plume of an Athena II SRM. No such in situ measurements of HNO_3 and NO_y have been reported previously. These measurements are used to calculate an NO_y emission index for the SRM and to infer the occurrence of (R1) on SRM-emitted alumina particles in the lower stratosphere.

2. Results and Discussion

[5] The Athena II SRM plume was sampled following launch from Vandenberg Air Force Base, CA (34°48′ N, 120°37′ W) on 24 September 1999 at 66060 s Universal Time (UT). In situ measurements were conducted onboard the NASA WB-57F high-altitude research aircraft as part of the NASA Atmospheric Chemistry of Combustion Emissions Near the Tropopause (ACCENT) mission. Species measured include NO and NO_y [*Weinheimer et al.*, 1993], HNO_3 [*Neuman et al.*, 2000], ClO [*Ross et al.*, 2000], carbon dioxide (CO_2) [*Gates et al.*, 2002], water vapor (H_2O) [*May*, 1998], and particles [*O. Schmid et al.*, manuscript in preparation, 2002]. The WB-57F rocket plume sampling methodology has been presented in detail elsewhere [*Ross et al.*, 1997a, 1997b]. The plume was sampled a total of 6 times, with the first 5 intercepts occurring at altitudes between 18.3 and 18.5 km in the

[1]Aeronomy Laboratory, National Oceanic and Atmospheric Administration, Boulder, CO, USA.
[2]Cooperative Institute for Research in Environmental Sciences, University of Colorado, Boulder, CO, USA.
[3]National Center for Atmospheric Research, Boulder, CO, USA.
[4]Laboratory for Atmospheric and Space Physics, University of Colorado, Boulder, CO, USA.
[5]Program in Atmospheric and Oceanic Sciences, University of Colorado, Boulder, CO, USA.
[6]The Aerospace Corporation, Los Angeles, CA, USA.
[7]Department of Engineering, University of Denver, Denver, CO, USA.
[8]Jet Propulsion Laboratory, California Institute of Technology, Pasadena, CA, USA.
[9]Atmospheric and Environmental Research, Inc., Lexington, MA, USA.

0094-8276/02/2002GL015197S05.00

lower stratosphere. The final plume encounter occurred at 16.5 km during the WB-57F final descent, and is not considered in any further analysis here.

2.1. NO_y Emission Index

[6] Time series measurements obtained during the 5 plume intercepts are shown in Figure 1. Plume ages, as measured from the time of emission, ranged from 3.8 to 26.3 min. The duration of the intercepts varied from 2.2 to 12.9 s, corresponding to flight paths of 0.4 to 2.1 km, respectively. To reach these dimensions, an SRM exhaust plume must undergo near-complete dilution with ambient air. NO_y, HNO_3, CO_2, and ClO mixing ratios, however, still increased substantially above background values in the plume. CO_2 values are shown as the amount above the stratospheric background value of approximately 368 ppmv. NO values in the plume as soon as 3.8 min after emission indicate a depletion from the background value of approximately 420 pptv to 125 pptv at the time of the first intercept and to smaller amounts in the remaining intercepts. This measurement illustrates the rapid chemical conversion of NO to higher oxides of nitrogen in the plume and emphasizes the importance of reporting an NO_y emission index using a measurement of all NO_y species.

[7] In calculating an NO_y emission index, the plume dilution and expansion exhibited in Figure 1 is accounted for by normalization to a conserved species with a known emission index such as CO_2. Since the SRM emission index of CO_2 is known to be 382 g (kg fuel)$^{-1}$, based on the carbon content of the fuel burned, measured NO_y can be directly related to fuel use by the relative abundances of NO_y and CO_2 in the plume. Comparing the emitted quantities of NO_y and CO_2 during the plume encounters shown in Figure 1 is accomplished by integrating both species after subtracting their respective background values. The integral comparisons are meaningful because each in situ measurement is made continuously or near-continuously in a constant sample flow [*Fahey et al.*, 1995a, 1995b].

[8] The plume-integrated values of NO_y and CO_2 (ΔNO_y and ΔCO_2, respectively) during each of the 5 plume intercepts are shown in Table 1. Although NO_y and CO_2 are conserved in the plume downstream of the afterburning region, the integrated values of both species vary by more than a factor of 2 during the 5 intercepts. This variance results from both the differences in the WB-57F flight paths within the plume, and the non-uniform dispersion of the plume in the lower stratosphere [*Beiting*, 2000]. Knowing ΔNO_y and ΔCO_2 for each plume intercept, the NO_y emission index, $EI(NO_y)$, can be calculated according to

$$EI(NO_y) = EI(CO_2) \cdot \frac{\Delta NO_y}{\Delta CO_2} \cdot \frac{46}{44} \text{ g } NO_2 \text{(kg propellant)}^{-1} \quad (1)$$

[*Fahey et al.*, 1995a] where $EI(CO_2)$ is the SRM CO_2 emission index and (46/44) represents the molar mass ratio of NO_y (expressed as equivalent mass of NO_2) to CO_2.

[9] Using equation 1, $EI(NO_y)$ values calculated for each of the 5 plume events yield an average of 2.7±0.6 g NO_2 (kg fuel)$^{-1}$ (Table 1). This value is higher than the prediction of 1.2 g NO_2 (kg fuel)$^{-1}$ calculated by one of the authors (P.F.Z.) using a plume flowfield model of the Athena II SRM initialized for conditions at 18.6 km altitude. For related

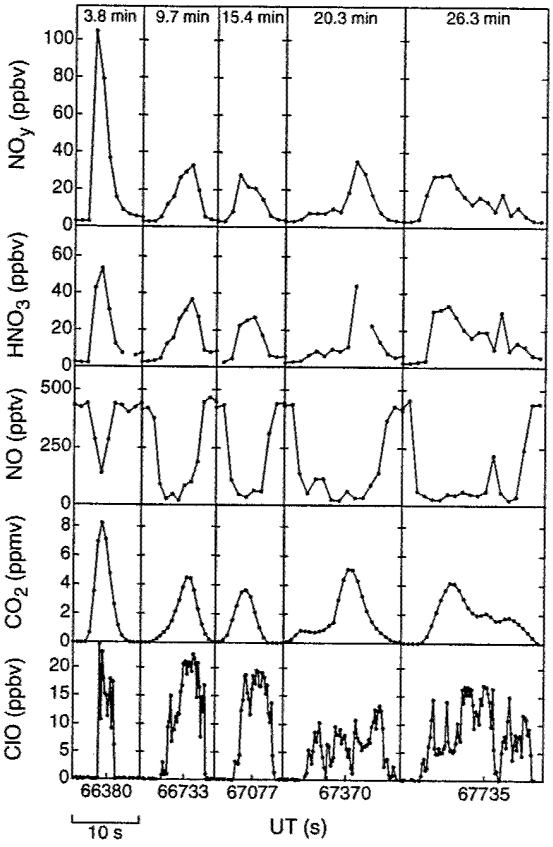

Figure 1. In situ measurements of NO_y, HNO_3, NO, CO_2, and ClO in the plume of an Athena II SRM launched from Vandenberg Air Force Base, CA on 24 September 1999 at 66060 UT. The panels showing data during the first plume intercept at 66380 UT represent 10 s of data. Panels for the remaining plume intercepts have the same horizontal scale. Plume ages at the time of intercept are shown at the top of each column.

examples of SRM plume chemistry calculations using supersonic SRM exhaust flowfield models, see *Zittel* [1994] and *Denison et al.* [1994]. Approximately 30% of the modeled NO production occurs in the SRM combustion chamber where the conditions affecting NO production are not well understood. The remaining NO production occurs primarily via the Zeldovich thermal mechanism [*Blazowski and Sawyer*, 1975] in the afterburning region of the plume and is highly sensitive to local temperature and mixing. Because of the uncertainties in afterburning plume conditions introduced by approximations to supersonic turbulent mixing, as well as the possibility that additional NO production paths may be discovered to be significant in the unusual SRM plume environment, the modeled NO production is considered an estimate and is easily subject to a factor of 2 uncertainty. While the model does not follow the reactions of NO subsequent to afterburning, the calculated NO residue can nonetheless be considered the sum of the NO_y species at all later times in the plume and is therefore directly comparable to the experimentally determined value. The comparable $EI(NO_y)$ values from the measurements and model predic-

Table 1. Details of the WB-57F Intercepts of the Athena II SRM Plume

Plume Int.	UT (s)	Age[a] (min)	T (K)	P (hPa)	TAS[b] (m/s)	Δt[c] (s)	ΔNO_y[d] (ppbv·s)	ΔCO_2[d] (ppmv·s)	EI(NO_y) (g NO_2/kg)	ΔHNO_3[d] (ppbv·s)	HNO_3/NO_y Observed	HNO_3/NO_y Lower Limit
1	66380	3.8	208	70	202	2.2	178	20.3	3.5	114	0.64	0.12
2	66733	9.7	208	69	191	5.7	125	17.8	2.8	147	1.18	0.23
3	67077	15.4	207	67	173	4.2	80	11.6	2.8	93	1.16	0.22
4	67370	20.3	207	69	181	8.7	122	24.6	2.0	152	1.25	0.24
5	67735	26.3	207	66	166	12.9	192	31.6	2.4	243	1.27	0.24

[a] Assumes passage of Athena II SRM through intercept altitudes at 66154 UT.
[b] True air speed of the WB-57F at the time of the plume intercept.
[c] Elapsed time of the plume intercept, defined as the full-width at half-maximum of the ClO instrument response in the plume.
[d] Δ indicates plume-integrated value with background atmospheric values subtracted. At intercept altitudes, the fuel mass flow rate of the Athena II SRM second stage was 590 kg s^{-1}, the vertical velocity was 396 m s^{-1} and the flight path angle was 48° from vertical.

tions represent satisfactory agreement considering the uncertainties in simulating the combustion chamber and afterburning plume conditions responsible for NO production.

2.2. HNO_3 Production

[10] The relative plume-integrated values of HNO_3 (ΔHNO_3) and NO_y shown in Table 1 indicate that HNO_3 is a significant and evolving component of NO_y in the aging rocket plume. The amount of HNO_3 produced within the SRM and the afterburning plume is uncertain and is not addressed directly by the plume flowfield model. Nonetheless, any increase in HNO_3 observed during the sampling passes must be produced in situ in the plume. It is also possible that all of the HNO_3 is formed in this manner. Such production could occur in the gas phase or heterogeneously on emitted alumina particles. The most likely gas-phase production pathway,

$$NO_2 + OH \rightarrow HNO_3 \qquad (R2)$$

is expected to be negligible, since it requires OH to be in excess of 1 ppbv to produce nominal HNO_3 values. Although there are no direct measurements of OH in the Athena II plume, the flowfield model predicts a negligible residue of OH in the cool plume. If the model is accurate, the OH density is too low by several orders of magnitude to explain the observed levels of HNO_3.

[11] The heterogeneous production of HNO_3 has been demonstrated in laboratory studies to occur via (R1) on the surface of alumina particles [*Molina et al.*, 1997]. NO produced directly by the SRM would be very short lived in the young (<3.8 min old) plume and efficiently converted to $ClONO_2$. Measurements in the plume indicate that less than 0.1% of the emitted NO remains after 3.8 min, while at the same time NO_y levels exceed 100 ppbv (Figure 1). This rapid NO removal likely occurs by reaction with ClO in the plume:

$$NO + ClO \rightarrow NO_2 + Cl \qquad (R3)$$

With 15 ppbv of ClO present (the approximate mean abundance of ClO in the plume during the first intercept, see Figure 1), the lifetime of NO in (R3) is approximately 1 s. The subsequent formation of $ClONO_2$, via

$$NO_2 + ClO \xrightarrow{M} ClONO_2 \qquad (R4)$$

results in an NO_2 lifetime of approximately 23 s. It should be noted that the lifetimes of NO and NO_2 stated here are upper limit estimates, considering that the ClO abundance early in the plume was likely higher than the measured value of 15 ppbv at 3.8 min. The net result of (R3) and (R4) is that NO_y not already in the form of HNO_3 is rapidly sequestered into the relatively stable reservoir species $ClONO_2$ in the young SRM plume. Using a reaction probability of 0.02 for (R1) [*Molina et al.*, 1997], and an observed alumina particle surface area density in the plume of $1.8 \cdot 10^3$ μm^2 cm^{-3} (data not shown), the lifetime of $ClONO_2$ through (R1) in the young plume is 8.6 min. Thus, substantial HNO_3 can be produced via (R1) in the Athena II SRM plume by the time of the first intercept at a plume age of 3.8 min.

[12] The observed HNO_3 to NO_y ratio is 0.64 during the first plume encounter and increases above unity for the remaining intercepts (Table 1). Although the increases above unity are within the combined uncertainty of the measurements, ratios less than or equal to one are expected based on measurements made prior to the plume intercepts and during a previous flight [*Neuman et al.*, 2000]. The HNO_3 to NO_y ratios greater than unity observed here are interpreted to be the result of some fraction of the HNO_3 being adsorbed on alumina particles present in the exhaust plume. Size-resolved measurements of particles in the plume, assumed to be composed of alumina, indicate a tri-modal distribution of particle surface area (SA) in the plume. The largest particle mode, representing 65% of the surface area in the plume, consists of particles with a mean diameter of 1.7 μm. The remaining particle surface area in the plume resides in smaller modes at 0.08 μm and 0.16 μm [*O. Schmid et al.*, manuscript in preparation, 2002].

[13] The HNO_3 instrument samples through a forward-facing, sub-isokinetic inlet, which causes particles larger than approximately 0.1 μm in diameter to be significantly enhanced in the sample flow [e.g. *Northway et al.*, 2002]. In contrast, little to no particle enhancement is expected in the side-facing NO_y inlet. Thus, if HNO_3 is adsorbed on alumina particles, the observed HNO_3 mixing ratio in the plume may exceed that of NO_y when HNO_3 constitutes a significant fraction of the NO_y present. A lower limit for the HNO_3 to NO_y ratio in the plume is derived by assuming that all HNO_3 in the plume is adsorbed on alumina particles. Using a calculated enhancement function for the HNO_3 inlet [e.g. *Northway et al.*, 2002] to adjust for particle enhancement, the lower limit ratio ranges from 0.12 at a plume age of 3.8 min to 0.24 at a plume age of 26.3 min (Table 1). If any HNO_3 is in the gas phase the effect of particle enhancement will be reduced, and the HNO_3 to NO_y ratio will be greater than the lower limit values and approach the observed ratios. The actual HNO_3 to NO_y ratio can only approach unity if almost all HNO_3 in the plume is in the gas phase and the effect of particle enhancement is minimized.

[14] The increase in the HNO_3 to NO_y ratio observed in the plume between the first and second plume encounters is

likely due to continued in situ production of HNO_3. Although there is uncertainty in the effective surface area density in the plume, the lifetime of $ClONO_2$ in the production of HNO_3 is long enough that (R1) could still be occurring. The near-constant HNO_3 to NO_y ratios after the second encounter are likely due to the cessation of HNO_3 production in the plume. Cessation could occur if $ClONO_2$ is completely converted to HNO_3 or if (R1) slows due to contamination of the alumina surface by adsorbed HNO_3, as suggested by *Molina et al.* [1997].

[15] As a final consideration, we note that nitric acid trihydrate (NAT; $HNO_3 \cdot 3H_2O$) is not stable in the aging plume. Water vapor mixing ratios are near 20 ppmv during the first plume intercept and 11–15 ppmv for the later crossings (data not shown). For 20 ppmv H_2O and the measured plume temperature of 208 K at 70 hPa, HNO_3 mixing ratios must exceed approximately 140 ppbv for NAT to be stable [*Hanson and Mauersberger*, 1988]. This value far exceeds the maximum HNO_3 mixing ratio of 51 ppbv observed during the first plume intercept. As H_2O mixing ratios drop to 11–15 ppbv in the later plume crossings, NAT continues to be unstable at the observed HNO_3 mixing ratios. Before the first crossing (at a plume age of 3.8 min), NAT may have been thermodynamically stable for a brief period in the expanding plume because the plume cools to ambient temperatures in a few seconds and the HNO_3 saturation mixing ratio depends non-linearly on the H_2O mixing ratio. In addition, NAT would be present at all the plume crossings if the ambient temperatures were slightly lower. Comprehensive plume models should include the possibility of NAT formation and the associated heterogeneous reactions on NAT particles.

3. Implications

[16] The results presented here provide the first measurements of the NO_y emission index for an SRM, highlighting the importance of validating the parameterizations and assumptions used in afterburning models. The accumulation of NO_y emitted by SRMs could potentially affect O_3 production and loss processes in the stratosphere. A typical SRM launch scenario described by *Danilin et al.* [2001] results in the combustion of $3.4 \cdot 10^6$ kg of fuel in the stratosphere annually. The calculated NO_y emission index of 2.7±0.6 g NO_2 (kg fuel)$^{-1}$ presented here, therefore, results in the annual emission of $9.2 \cdot 10^3$ kg of NO_y directly into the stratosphere. In contrast, the production of reactive nitrogen in the stratosphere from the decomposition of N_2O is approximately $1.5 \cdot 10^9$ kg NO_2 yr^{-1} [*Murphy and Fahey*, 1994]. Thus, the contribution of SRM emissions to the stratospheric NO_y budget is negligible compared to that from natural sources. Future NO_y emissions from other rocket propellant types (i.e. hydrazine-based fuels) may not be negligible.

[17] These data also provide the first experimental evidence for the production of HNO_3 via (R1) on SRM-emitted alumina particles in the lower stratosphere. In addition, they provide evidence that HNO_3 may remain adsorbed on the alumina particles. Although the occurrence of (R1) results in chlorine activation in the plume, the importance for local O_3 loss is not clear since active chlorine is otherwise abundant in the plume [*Ross et al.*, 1997a, 1997b]. With the potential future increase in launch vehicle traffic, understanding how reactions on alumina particles affect global stratospheric O_3 will be critical in assessing the effects of the space launch industry.

[18] **Acknowledgments.** The authors wish to thank the air and ground crews of the NASA WB-57F aircraft. This work was supported in part by the NASA Atmospheric Effects of Aviation Project. NCAR is supported by the National Science Foundation. Part of the work described in this paper was carried out by the Jet Propulsion Laboratory, California Institute of Technology, under contract with the National Aeronautics and Space Administration.

References

Blazowski, W. S., and R. F. Sawyer, Fundamentals of pollutant formation, in Propulsion Effluents in the Stratosphere, Monograph 2, *Rep. DOT-TST-75-52*, pp. (4–1)–(4–52), U.S. Dept. of Trans., Washington D.C., 1975.

Beiting, E. J., Measurements of stratospheric plume dispersion by imagery of solid rocket motor exhaust, *J. Geophys. Res.*, *105*, 6891–6901, 2000.

Bennet, R. R., and A. J. McDonald, The atmospheric impacts of chemical rocket motors, in *Impact of emissions from aircraft and spacecraft upon the atmosphere*, edited by U. Schumann and D. Wurzel, pp 378–383, Cologne, Germany, 1994.

Danilin, et al., Global stratospheric effects of the alumina emissions by solid-fueled rocket motors, *J. Geophys. Res.*, *106*, 12,727–12,738, 2001.

Denison, M. R., et al., Solid rocket exhaust in the stratosphere: Plume diffusion and chemical reactions, *J. Spacecr. Rockets*, *31*, 435–442, 1994.

Fahey, D. W., et al., In situ observations in aircraft exhaust plumes in the lower stratosphere at midlatitudes, *J. Geophys. Res.*, *100*, 3065–3074, 1995a.

Fahey, D. W., et al., Emission measurements of the Concorde supersonic aircraft in the lower stratosphere, *Science*, *270*, 70–74, 1995b.

Gates, A. M., et al., In-situ measurements of carbon dioxide, 0.37–4.0 μm particles, and water vapor in the stratospheric plumes of three rockets, *J. Geophys. Res.*, In press, 2002.

Hanson, D., and K. Mauersberger, Laboratory studies of the nitric acid trihydrate: Implications for the south polar stratosphere, *Geophys. Res. Lett.*, *15*, 855–858, 1988.

May, R. D., Open-path, near-infrared tunable diode laser spectrometer for the atmospheric measurement of H_2O, *J. Geophys. Res.*, *103*, 19,161–19,172, 1998.

Molina, M. J., et al., The reaction of $ClONO_2$ with HCl on aluminum oxide, *Geophys. Res. Lett.*, *24*, 1619–1622, 1997.

Murphy, D. M., and D. W. Fahey, An estimate of the flux of stratospheric reactive nitrogen and ozone into the troposphere, *J. Geophys. Res.*, *99*, 5325–5332, 1994.

Neuman, J. A., et al., A fast-response chemical ionization mass spectrometer for in-situ measurements of HNO_3 in the upper troposphere and lower stratosphere, *Rev. Sci. Instrum.*, *71*, 3886–3894, 2000.

Northway, M. J., et al., An analysis of large HNO_3-containing particles sampled in the Arctic stratosphere in the winter of 1999–2000, *J. Geophys. Res.*, In press, 2002.

Potter, A. E., Proceedings of the space shuttle environmental assessment workshop on stratospheric effects, *NASA TM X-58,198, App. G*, National Aeronautics and Space Administration, Washington D.C., 1977.

Prather, M. J., et al., The Space Shuttle's impact on the stratosphere, *J. Geophys. Res.*, *95*, 18,583–18,590, 1990.

Ross, M. N., et al., In-situ measurement of Cl_2 and O_3 in a stratospheric solid rocket motor exhaust plume, *Geophys. Res. Lett.*, *24*, 1755–1758, 1997a.

Ross, M. N., et al., Observation of stratospheric ozone depletion in rocket exhaust plumes, *Nature*, *390*, 62–64, 1997b.

Ross, M. N., et al., Observations of stratospheric ozone depletion associated with Delta II rocket emissions, *Geophys. Res. Lett.*, *27*, 2209–2212, 2000.

Weinheimer, A. J., et al., Stratospheric NO_y measurements on the NASA DC-8 during AASE II, *Geophys. Res. Lett.*, *22*, 2563–2566, 1993.

Zittel, P. F., Computer model predictions of the local effects of large solid-fueled rocket motors on stratospheric ozone, *Tech. Rep. TR-94(4231)-9*, Aerospace Corp., El Segundo, CA, 1994.

P. J. Popp, R. S. Gao, J. A. Neuman, M. J. Northway, J. C. Holecek, D. W. Fahey, T. L. Thompson, and K. K. Kelly, Aeronomy Laboratory, National Oceanic and Atmospheric Administration, Boulder, CO 80305, USA. (ppopp@al.noaa.gov)

B. A. Ridley, J. G. Walega, and F. E. Grahek, National Center for Atmospheric Research, Boulder, CO 80307, USA.

L. M. Avallone, Laboratory for Atmospheric and Space Physics, University of Colorado, Boulder, CO 80309, USA.

D. W. Toohey, Program in Atmospheric and Oceanic Sciences, University of Colorado, Boulder, CO 80309, USA.

P. F. Zittel and M. N. Ross, The Aerospace Corporation, Los Angeles, CA 90009, USA.

O. Schmid and J. C. Wilson, Department of Engineering, University of Denver, Denver, CO 80208, USA.

R. L. Herman, Jet Propulsion Laboratory, California Institute of Technology, Pasadena, CA 91109, USA.

M. Y. Danilin, AER Inc., Lexington, MA 02421, USA.